DOI: 10.1534/genetics.106.056465

Identification and Classification of Genes That Act Antagonistically to *let-60* Ras Signaling in *Caenorhabditis elegans* Vulval Development

Craig J. Ceol,[1] Frank Stegmeier,[2] Melissa M. Harrison and H. Robert Horvitz[3]

Department of Biology, Howard Hughes Medical Institute, Massachusetts Institute of Technology, Cambridge, Massachusetts 02139

Manuscript received January 28, 2006
Accepted for publication April 2, 2006

ABSTRACT

The synthetic multivulva (synMuv) genes negatively regulate Ras-mediated vulval induction in the nematode *Caenorhabditis elegans*. The synMuv genes define three classes, A, B, and C, such that double mutants carrying mutations in genes of any two classes are multivulva. The class B synMuv genes include *lin-35*, a homolog of the retinoblastoma (Rb) tumor suppressor gene, as well as homologs of genes that function with Rb in transcriptional regulation. We screened for additional synMuv mutations using a strategy different from that of previous synMuv genetic screens. Some of the mutations we recovered affect new synMuv genes. We present criteria for assigning synMuv mutations into different genetic classes. We also describe the molecular characterization of the class B synMuv gene *lin-65*.

A fundamental issue in developmental biology is how cells that are initially equivalent in developmental potential ultimately adopt different fates. Genetic studies have indicated that cells within a developmental equivalence group often adopt different fates in response to the combined action of multiple and sometimes competing signals (reviewed by Freeman and Gurdon 2002). For example, the initial step of R8 photoreceptor specification in ommatidial development in *Drosophila melanogaster* uses both positive and negative signals to properly select presumptive R8 photoreceptors from a field of developmentally equivalent cells in the eye imaginal disc (reviewed by Frankfort and Mardon 2002). An overlay of such signals can make a response in binary cell-fate decisions more precise or can increase the number of fates available to a particular cell.

Vulval development in the nematode *Caenorhabditis elegans* involves a set of ectodermal P*n*.p cells that initially have similar developmental potentials but ultimately adopt different fates (Kimble 1981; Sternberg and Horvitz 1986). The specification of P*n*.p cells that eventually make vulval tissue occurs in two steps, each of which involves the selection of a subset of P*n*.p cells from a larger P*n*.p field (Sulston and Horvitz 1977). First, in the L1 larval stage shortly after the 12 P*n*.p cells are generated, the P1.p and P2.p anterior and P(9–11).p posterior cells fuse with the syncytial hypodermis. Each of the six remaining unfused midbody cells P(3–8).p has the capacity to adopt a vulval cell fate (Sternberg and Horvitz 1986). Second, three of these six cells, P(5–7).p, adopt vulval fates and undergo three rounds of division to generate seven (P5.p and P7.p) or eight (P6.p) descendants. P3.p, P4.p, and P8.p adopt nonvulval fates, typically dividing only once to generate two descendants that eventually fuse with the syncytial hypodermis. The decision to adopt vulval cell fates occurs during the L2 and early L3 larval stages and is followed by cell divisions and differentiation in the L3 and L4 larval stages, respectively (Kimble 1981; Sternberg and Horvitz 1986; Ferguson *et al.* 1987).

Many genes that control the specification of P*n*.p fates have been identified. Some of these genes act in a spatially restricted fashion to select P*n*.p cells for vulval development. The homeobox gene *lin-39* is expressed in the midbody and regulates the sequential steps of fusion and vulval cell-fate specification of the P*n*.p cells in this region (Clark *et al.* 1993; Wang *et al.* 1993; Maloof and Kenyon 1998). Strong loss-of-function *lin-39* mutations result in ectopic P(3–8).p cell fusion during the L1 stage. In partial loss-of-function *lin-39* mutants, unfused P(5–7).p cells are sometimes observed and often show vulval-to-non-vulval cell-fate transformations (Clark *et al.* 1993). *lin-39* activity therefore promotes unfused cell fates in the L1 stage and vulval cell fates in the L2 and early L3 stages. Genes in the *let-60* Ras signaling pathway also regulate the specification of P*n*.p fates (Beitel *et al.* 1990; Han and Sternberg 1990). In addition to *let-60* Ras, this pathway includes the receptor tyrosine kinase *let-23*, the SH2/SH3 adaptor *sem-5*, and the MAP kinase *mpk-1*, all of which are

Sequence data from this article have been deposited with the EMBL/GenBank Data Libraries under accession nos. AY818712 and AY818713.

[1]*Present address:* Howard Hughes Medical Institute, Department of Hematology/Oncology, Children's Hospital, Boston, Massachusetts 02115.

[2]*Present address:* Howard Hughes Medical Institute, Department of Genetics, Harvard Medical School, Boston, Massachusetts 02115.

[3]*Corresponding author:* Department of Biology, Howard Hughes Medical Institute, Massachusetts Institute of Technology, 77 Massachusetts Ave., Room 68-425, Cambridge, MA 02139. E-mail: horvitz@mit.edu

broadly conserved in Ras signaling systems (reviewed by Moghal and Sternberg 2003). The role of *let-60* Ras signaling in the specification of vulval cell fates is well characterized. In wild-type animals, the *let-60* Ras pathway is specifically activated in P(5–7).p in response to an EGF-like signal, encoded by *lin-3*, that is produced by the neighboring gonadal anchor cell (Hill and Sternberg 1992). Mutations that reduce *let-60* Ras pathway activity prevent P(5–7).p vulval cell-fate specification, resulting in a vulvaless (Vul) phenotype. Mutations that abnormally activate this pathway cause P(3–8).p all to adopt vulval cell fates, resulting in a multivulva (Muv) phenotype (Beitel *et al.* 1990; Han and Sternberg 1990; Eisenmann and Kim 1997). Increases in *let-60* Ras pathway activity may promote vulval cell fates in part by upregulating *lin-39* expression (Maloof and Kenyon 1998).

The activities of *lin-39* and genes in the *let-60* Ras pathway are antagonized by the synthetic multivulva (synMuv) genes. The synMuv genes define three redundant classes, A, B, and C (Ferguson and Horvitz 1989; Thomas *et al.* 2003; Ceol and Horvitz 2004). Animals carrying mutations affecting any two classes of synMuv genes are Muv, but animals with a mutation in one synMuv gene or in multiple synMuv genes of a single class undergo wild-type vulval development. All three classes of genes promote the expression of nonvulval cell fates by P(3–8).p. At present it is unknown whether the synMuv mutations cause an increase of *let-60* Ras pathway activity in these cells or cause these cells to be more sensitive to normal levels of *let-60* Ras pathway activity. Roles for synMuv genes in regulating P*n*.p fusion have also been described. Some class B genes, but no class A genes, antagonize *lin-39*-mediated cell fusion of at least one P*n*.p cell, P3.p (Chen and Han 2001).

Many synMuv genes have been molecularly characterized. The class B synMuv protein LIN-35 is similar to the mammalian tumor suppressor pRb (Lu and Horvitz 1998). Other class B synMuv proteins include DPL-1 and EFL-1, which are similar to mammalian DP and E2F proteins and, by analogy to their mammalian counterparts, likely function to target LIN-35 retinoblastoma (Rb) to DNA (Ceol and Horvitz 2001). The class B synMuv protein HDA-1 is similar to class I histone deacetylases (Lu and Horvitz 1998) and may be targeted to specific genes by a DPL-1/EFL-1/LIN-35-containing protein complex.

As *lin-35* Rb can act in the surrounding hypodermis to regulate P(3–8).p fates, the genes targeted by a DPL-1/EFL-1/LIN-35-containing complex may function noncell autonomously to regulate the specification of vulval cell fates (Myers and Greenwald 2005). Other class B synMuv proteins also are components of this complex (M. M. Harrison and H. R. Horvitz, unpublished observations), and complexes purified from Drosophila extracts containing DP, E2F, and Rb homologs contain homologs of the synMuv proteins LIN-9, LIN-37, LIN-52, LIN-53 RbAp48, LIN-54, and LIN-61 (Korenjak *et al.* 2004; Lewis *et al.* 2004). These Drosophila complexes can repress transcription of DP/E2F target genes and can inhibit genomewide DNA replication in ovarian somatic follicle cells.

The class C synMuv genes encode components of a putative histone acetyltransferase complex similar to the human Tip60 and yeast NuA4 histone acetyltransferase complexes (Ceol and Horvitz 2004). The molecular identities of class B and class C synMuv genes suggest that chromatin remodeling and modification are important in specifying P(3–8).p fates. The class A synMuv genes *lin-15A* and *lin-8* encode novel proteins (Clark *et al.* 1994; Huang *et al.* 1994; Davison *et al.* 2005). Little is known about the mechanism of action of the class A synMuv genes.

Previous synMuv genetic screens required that mutant isolates be fertile for the recovery of synMuv mutations. We used a screening approach that allowed the recovery of synMuv mutations that cause recessive sterility. We describe the characterization of new synMuv mutations and criteria used to distinguish new and previously described classes of synMuv genes.

MATERIALS AND METHODS

Strains and general techniques: Strains were cultured as described by Brenner (1974) and grown at 20° unless otherwise indicated. The wild-type parent of all *C. elegans* strains described in this study was the Bristol strain N2, except that some multifactor mapping experiments used the polymorphic wild-type strains RW7000 (Williams *et al.* 1992) and CB4856 (Wicks *et al.* 2001). We also used strains containing the following mutations:

LGI: *bli-3(e767)*, *lin-17(n677)*, *unc-11(e47)*, *unc-73(e936)*, *lin-44(n1792)*, *unc-38(x20)*, *dpy-5(e61)*, *lin-35(n745)*, *unc-13(e1091)*, *lin-53(n833)* (Ferguson and Horvitz 1989), and *unc-54(e1092)* (Dibb *et al.* 1985).

LGII: *lin-31(n301)*, *dpy-10(e128)*, *tra-2(q276)*, *rol-6(e187)*, *dpl-1(n2994)* (Ceol and Horvitz 2001; Thomas *et al.* 2003), *let-23(sy10, sy97)*, *unc-4(e120)*, *unc-53(n569)*, *mex-1(it9)*, *rol-1(e91)*, and *lin-38(n751)*.

LGIII: *dpy-17(e164)*, *lon-1(e185)*, *lin-13(n770)* (Ferguson and Horvitz 1989), *lin-37(n758)*, *lin-36(n766)*, *unc-36(e251)*, *lin-9(n112)*, *unc-32(e189)*, *lin-52(n771)* (Ferguson and Horvitz 1989), and *dpy-18(e364)*.

LGIV: *lin-1(e1275)*, *unc-5(e53)*, *unc-24(e138)*, *mec-3(e1338)*, *lin-3(n378)*, *sem-3(n1900)* (M. J. Stern and H. R. Horvitz, unpublished results), *dpy-20(e1282)*, *unc-22(e66)*, *dpy-26(n198)*, *ark-1(sy247)* (Hopper *et al.* 2000), *unc-31(e169)*, *unc-30(e191)*, *lin-54(n2231)* (Thomas *et al.* 2003), and *dpy-4(e1166)*.

LGV: *tam-1(cc567)* (Hsieh *et al.* 1999), *unc-46(e177)*, *let-418 (s1617)*, *dpy-11(e224)*, *rol-4(sc8)*, *unc-76(e911)*, *efl-1(n3318)* (Ceol and Horvitz 2001), and *dpy-21(e428)*.

LGX: *egl-17(e1313)*, *sli-1(sy143)*, *aex-3(ad418)*, *unc-1(e1598 n1201)* (E. C. Park and H. R. Horvitz, unpublished results), *dpy-3(e27)*, *gap-1(ga133)* (Hajnal *et al.* 1997), *unc-2(e55)*, *lon-2(e678)*, *unc-10(e102)*, *dpy-6(e14)*, *unc-9(e101)*, *unc-3(e151)*, *lin-15B(n744)*, *lin-15A(n767)*, and *lin-15AB(n765)*.

Unless otherwise noted, the mutations used are described by Hodgkin (1997). In addition, we used strains containing

the following chromosomal aberrations: *mnDf57 II* (Sigurdson *et al.* 1984), *mnDf90 II* (Sigurdson *et al.* 1984), *mnDf29 II* (Sigurdson *et al.* 1984), *mnDf87 II* (Sigurdson *et al.* 1984), *mIn1[dpy-10(e128) mIs14] II* (Edgley and Riddle 2001), *mnC1[dpy-10(e128) unc-52(e444)] II* (Herman 1978), *nDf40 III* (Hengartner *et al.* 1992), *qC1[dpy-19(e1259) glp-1(q339)] III* (Austin and Kimble, 1989), *sDf63 IV* (Clark and Baillie 1992), *sDf62 IV* (Clark and Baillie 1992), *sDf10 IV* (Rogalski *et al.* 1982), *hT2[qIs48] (I;III)* (L. Mathies and J. Kimble, personal communication), *eT1(III;V)* (Rosenbluth and Baillie 1981), *nT1(IV;V)* (Ferguson and Horvitz 1985), *nT1(n754) (IV;V)*, and *nT1[qIs51] (IV;V)* (L. Mathies and J. Kimble, personal communication). *n754* causes a dominant Unc phenotype, allowing *nT1(n754)*-containing larvae and adults to be scored (E. L. Ferguson and H. R. Horvitz, unpublished results). *mIs14*, an integrated transgene linked to the chromosomal inversion *mIn1* (Edgley and Riddle 2001), and *qIs48* and *qIs51*, integrated transgenes linked to the reciprocal translocations *hT2(I;III)* and *nT1(IV;V)*, respectively (L. Mathies and J. Kimble, personal communication), consist of GFP-expressing transgenes that allow *mIs14*, *qIs48*, or *qIs51*-containing animals to be scored beginning at the four-cell stage of embryogenesis.

Isolation of new alleles: We mutagenized *lin-15A(n767)* hermaphrodites with ethyl methanesulfonate (EMS) as described by Brenner (1974). We allowed these animals to recover on food for between 15 min and 1 hr and then transferred individual P_0 larvae in L4 lethargus to 50-mm petri plates. After 3–5 days, 20 F_1 L4 larvae per P_0 were individually transferred to 50-mm plates, and F_2 animals on these plates were subsequently screened for a Muv phenotype. We screened the progeny of 3380 F_1 animals using this procedure.

Linkage group assignment: We mapped newly isolated synMuv mutations to linkage groups using standard methods (Brenner 1974), except for some mutations that we mapped using the polymorphisms present in the wild-type strain RW7000 (Williams *et al.* 1992).

Complementation tests: We performed complementation tests as described by Ferguson and Horvitz (1989). Hemizygous *lin-15B(n3711) lin-15A(n767)* males could not mate. To perform complementation tests with this mutation, we mated *tra-2(q276); lin-15B(n3711) lin-15A(n767)/++* XX males with marked *lin-15AB* hermaphrodites and scored cross-progeny.

Construction of deficiency heterozygotes: To construct *trr-1(n3712)* heterozygotes with the *mnDf57*, *mnDf90*, and *mnDf29* deletions, *Df/mIn1; lin-15A(n767)* males were generated. These males were mated with *rol-6 trr-1(n3712)/mIn1; lin-15A(n767)* hermaphrodites, and non-Rol, non-Gfp cross-progeny were scored. *mnDf87* heterozygous males do not mate, so in this case we generated *trr-1(n3712)/mnDf87; lin-15A(n767)* animals by mating *trr-1(n3712)/mIn1; lin-15A(n767)* males with *unc-4 mnDf87/mIn1; lin-15A(n767)* hermaphrodites. *mep-1/Df* animals were constructed by mating *Df/nT1; +/nT1* males with *dpy-20 mep-1; lin-15A(n767)* hermaphrodites and scoring non-Dpy cross-progeny.

Construction of single-mutant and unlinked double-mutant strains: The synMuv mutations listed below were balanced in *trans* by the specified double-mutant combinations or chromosomal aberrations in constructing strains with a single synMuv mutation or strains carrying two unlinked synMuv mutations:

lin-65(n3441): *bli-3(e767) lin-17(n677), hT2[qIs48] (I;III).*
lin(n3628): *unc-11(e47) dpy-5(e61), hT2[qIs48] (I;III).*
lin-35(n745): *dpy-5(e61) unc-13(e1091), hT2[qIs48] (I;III).*
trr-1(n3712): *mIn1[dpy-10(e128) mIs14].*
lin-38(n751): *mnC1[dpy-10(e128) unc-52(e444)].*
mep-1(n3703): *dpy-20(e1282) unc-30(e191), nT1 n754 (IV;V), nT1[qIs51] (IV;V).*
ark-1(n3701): *dpy-20(e1282) unc-30(e191), nT1 n754 (IV;V), nT1[qIs51] (IV;V).*
mys-1(n3681): *unc-46(e177) dpy-11(e224), nT1 n754 (IV;V), nT1[qIs51] (IV;V).*
let-23(sy97) was balanced with *mIn1[dpy-10(e128) mIs14].*

A *sli-1* single mutant was constucted by generating *+ sli-1 + lin-15A/egl-17 + unc-1 +* hermaphrodites and identifying non-mutant progeny that segregated only Egl Unc non-Muv and non-Egl non-Unc non-Muv animals. Non-Egl non-Unc non-Muv animals were isolated, and *sli-1* homozygotes were identified as those that did not segregate Egl Unc non-Muv progeny. Double-mutant strains containing an X-linked mutation in *sli-1*, *gap-1*, *lin-15A*, or *lin-15B* and an autosomal mutation were constructed essentially as described by Ferguson and Horvitz (1989).

To ensure that mutations were not lost by recombination, several independent lines were isolated for each strain. Some double-mutant strains that exhibited a strong synMuv phenotype were constructed on the basis of their Muv phenotype without the use of balancers.

Construction of linked double-mutant strains: To construct an *n3628 lin-35* double mutant, hermaphrodites of genotype *n3628 dpy-5 + +/+ + lin-35 unc-13; lin-15A* were generated. Muv non-Dpy non-Unc progeny that segregated only Muv non-Dpy non-Unc, Muv Dpy non-Unc, and Muv Unc non-Dpy animals were selected. Muv Unc non-Dpy animals of the genotype *n3628 lin-35 unc-13; lin-15A* were isolated, and the *lin-15A* mutation was crossed out using *unc-11 dpy-5* as a balancer.

To construct a *sli-1 lin-15B* double mutant, *+ sli-1 + lin-15A/egl-17 + unc-1 lin-15AB* hermaphrodites were generated. Muv non-Egl non-Unc progeny that segregated only Muv non-Egl non-Unc and Muv Egl Unc animals were selected. Muv non-Egl non-Unc animals of the genotype *sli-1 lin-15AB* were isolated. From these animals, *+ sli-1 + lin-15AB/egl-17 + unc-1 lin-15B* animals were generated. non-Muv non-Egl non-Unc progeny that segregated only non-Muv non-Egl non-Unc and Egl Unc non-Muv animals were identified, and non-Muv non-Egl non-Unc animals of the genotype *sli-1 lin-15B* were isolated. A *gap-1 lin-15B* double mutant was similarly constructed using *dpy-3 unc-2* as a balancer.

A *sli-1 gap-1* double mutant was constructed by generating *sli-1 + dpy-3 +/+ unc-1 + gap-1* hermaphrodites and individually isolating non-Dpy non-Unc progeny. Progeny that segregated only non-Dpy non-Unc and Dpy non-Unc animals were identified, and non-Dpy non-Unc animals of the genotype *sli-1 gap-1* were subsequently isolated.

Because *trr-1(n3712)* and *let-23(sy97)* cause recessive sterility and highly penetrant larval lethality, respectively, we could not isolate *trr-1* or *let-23* homozygotes in our construction of a *trr-1 let-23* double mutant. For this reason, we built this double mutant by first generating *+ rol-6 + trr-1/let-23 + unc-4 +; lin-15A* males and mating them with *mIn1[dpy-10(e128) mIs14]; lin-15A* hermaphrodites. Non-Dpy cross-progeny were individually isolated. Non-Dpy progeny with broods consisting of dead larvae and Vul Unc Gro non-Muv non-Rol non-Gfp and Gfp non-Vul non-Unc non-Gro non-Rol animals were identified. The presence of *trr-1* in these broods, as judged by the *trr-1*-associated growth-rate abnormality (Gro), was later confirmed by complementation testing. *lin-15A* was crossed out to generate a *let-23 unc-4 trr-1/ mIn1[dpy-10(e128) mIs14]* strain.

Assay for P(3–8).p vulval cell fates: Cell fates were scored in L4 hermaphrodites using Nomarski microscopy by counting the number of descendants that had been produced by individual P(3–8).p cells. Scores of 1, 0.5, and 0 were assigned to cells that did fully, partially, or not adopt vulval cell fates, respectively. P(3–8).p cells that partially adopt a vulval cell fate have one daughter that divides to produce two to four descendants and another daughter that remains undivided (Aroian and Sternberg 1991).

RNA-mediated interference: Templates for *in vitro* transcription reactions were made by PCR amplification of cDNAs and their flanking T3 and T7 promoter sequences. *In vitro* transcribed RNA was denatured for 10 min and subsequently annealed prior to injection.

***lin-65* rescue:** Using Gateway *in vitro* recombination technology (Invitrogen, San Diego), we cloned the open reading frame encoding the 728-amino-acid LIN-65 protein from a pENTR201*lin-65* entry clone into the pMB1 and pMB7 destination vectors. pMB1 and pMB7 (kindly provided by M. Boxem and S. van den Heuvel) are designed to express inserted sequences under the control of the *C. elegans* heat-shock protein promoters P_{hsp}16-2 and P_{hsp}16-41, respectively. We performed transformation rescue (Mello *et al.* 1991) using the green fluorescent protein-expressing plasmid pTG96 (kindly provided by Min Han) as a coinjection marker. Transgenic animals were heat-shocked as L1 and L2 larvae for 1 hr at 33° and scored as adults. Control transgenic animals were not heat-shocked.

Allele sequence: We used PCR-amplified regions of genomic DNA as templates in determining gene sequences. For each gene investigated, we determined the sequences of all exons and splice junctions. Whenever observed, the sequence of a mutation was confirmed using an independently derived PCR product. All sequences were determined using an automated ABI 373 DNA sequencer (Applied Biosystems, Foster City, CA).

RESULTS

Isolation of new synMuv mutants: A severe reduction of class B synMuv gene function is often associated with sterility: (1) In a genetic screen for alleles that did not complement the synMuv phenotype of *lin-9(n112)*, Ferguson and Horvitz (1989) recovered two *lin-9* alleles, *n942* and *n943*, that caused recessive sterility; (2) gene-dosage studies indicate that, in comparison to the wild type, *lin-52(n771)/Df* and *dpl-1(n2994)/Df* heterozygotes have markedly reduced brood sizes (Ceol and Horvitz 2001; Thomas *et al.* 2003); and (3) deletion mutations of some synMuv genes recovered using a PCR-based screening approach show recessive sterility, *e.g.*, mutations of *lin-53* (Lu 1999), *efl-1*, and *dpl-1* (Ceol and Horvitz 2001).

Previous genetic screens for synMuv mutants (Ferguson and Horvitz 1989; Thomas *et al.* 2003) were performed before a connection between loss of synMuv gene function and sterility was well established. These screens required that isolates be fertile and viable for the recovery of mutant alleles and failed to recover mutations of the class B synMuv genes *efl-1* and *let-418*, both of which can mutate to cause a sterile phenotype (von Zelewsky *et al.* 2000; Ceol and Horvitz 2001). These results suggested that additional synMuv genes might be identified in a screen that allowed the recovery of homozygous sterile mutations.

To screen for new synMuv mutants, we examined the progeny of individual F_1 animals after EMS mutagenesis of their *lin-15A(n767)* parents. We screened the progeny of 3380 F_1 animals (6760 haploid genomes) for mutations that either alone or in combination with *lin-15A(n767)* caused a recessive Muv phenotype. Mutations that caused recessive sterility in addition to a Muv phenotype were recovered from their heterozygous wild-type siblings present on the same petri plate. Using this strategy we identified 95 Muv mutations, 24 of which we maintained as heterozygotes because of a recessive sterility that cosegregated with the Muv phenotype. Three mutations caused a Muv phenotype in the absence of *lin-15A(n767)* and were found to affect the previously studied genes *lin-1* and *lin-31*, both of which function downstream of *let-60* Ras in vulval induction (Ferguson *et al.* 1987). These mutations, *lin-1(n3443)*, *lin-1(n3522)*, and *lin-31(n3440)*, were not characterized further. Thirty mutations when in combination with *lin-15A(n767)* caused a weakly penetrant (<30%) Muv phenotype. We were unable to convincingly map these mutations to linkage groups. The remaining 62 mutations were assigned to 20 complementation groups (see below). Five of these mutations affect the synMuv gene *lin-61* and will be described elsewhere (M. M. Harrison, X. Lu and H. R. Horvitz, unpublished results).

Phenotypes of new mutants: We characterized the penetrance of the Muv phenotype of each strain at 15° and 20° (Table 1). At 25° the penetrance of each strain was between 98 and 100% ($n \geq 25$), except for *gap-1(n3535); lin-15A(n767)* (91%, $n = 111$) and *lin(n3542) lin-15A(n767)* (90%, $n = 42$). Since a heat-sensitive Muv phenotype is characteristic of most synMuv strains, including those with null mutations in synMuv genes, it is likely that many individual synMuv mutations are not temperature sensitive but rather that the synMuv genes regulate a temperature-sensitive process (Ferguson and Horvitz 1989).

As described in Table 1, many of these synMuv strains also exhibited a sterile phenotype. In these strains, the sterile phenotype cosegregated with the Muv phenotype during backcrosses and two- and three-factor mapping experiments. For *efl-1*, *let-418*, and certain *lin-9* and *lin-53* mutations, we found that our new mutations did not complement the sterile phenotypes caused by previously isolated allelic synMuv mutations (data not shown). Mutations defining new synMuv loci likewise failed to complement each other for the sterile phenotype: *mep-1(n3702)* did not complement *mep-1(n3703)*, and none of the other five *trr-1* mutations complemented *trr-1(n3712)* for the sterile phenotype. These observations indicate that the sterile and Muv phenotypes of these strains were caused by the same mutation.

New synMuv genes: Using two-factor crosses and X chromosome transmission tests (see materials and methods), we mapped the new mutations to linkage groups. We then determined if each mutation failed to complement mutations in known synMuv genes on the same linkage group. In these tests we identified 41 alleles of known synMuv genes: 1 *dpl-1*, 1 *efl-1*, 7 *let-418*, 3 *lin-9*, 4 *lin-13*, 10 *lin-15B*, 2 *lin-35*, 3 *lin-36*, 1 *lin-52*, 4 *lin-53*, and 5 *lin-61* mutations. We isolated 1 mutation in *gap-1* and 3 in *sli-1*, two genes that were originally

identified in screens for mutations that suppress the Vul phenotype caused by a reduction in *let-60* Ras pathway signaling (Jongeward *et al.* 1995; Hajnal *et al.* 1997). We also identified two mutations in *ark-1*, a gene first identified in a screen for mutations that cause ectopic vulval cell fates in a *sli-1* mutant background (Hopper *et al.* 2000). *gap-1*, *sli-1*, and *ark-1* single mutants were previously found to have no (*sli-1*, *gap-1*) or subtle (*ark-1*) defects in vulval development. Our results indicate that *sli-1*, *gap-1*, and *ark-1* act redundantly with *lin-15A* to negatively regulate *let-60* Ras signaling.

Mutations that were not assigned to known synMuv complementation groups were tested against unassigned mutations on the same linkage group for complementation. These tests defined five new synMuv loci: *lin-65*, *lin(n3628)*, *mep-1*, *mys-1*, and *trr-1*. [*lin(n3542)* may define another new synMuv locus, but since we have not separated *lin(n3542)* from *lin-15A(n767)*, we do not

TABLE 1

Phenotypes of synMuv mutant strains

Genotype	% Muv (*n*)		Additional abnormalities
	15°	20°	
ark-1(n3524); lin-15A(n767)	0 (251)	80 (171)	
ark-1(n3701); lin-15A(n767)	12 (190)	95 (160)	
dpl-1(n3643); lin-15A(n767)[a]	99 (154)	100 (252)	
efl-1(n3639); lin-15A(n767)[a]	93 (74)	100 (78)	Ste
gap-1(n3535) lin-15A(n767)	1 (143)	50 (236)	
let-418(n3536); lin-15A(n767)	0 (201)	55 (183)	hs Ste
let-418(n3626); lin-15A(n767)	2 (62)	97 (76)	Ste
let-418(n3629); lin-15A(n767)	0 (52)	86 (58)	Ste
let-418(n3634); lin-15A(n767)	0 (87)	92 (48)	Ste
let-418(n3635); lin-15A(n767)	0 (76)	71 (70)	Ste
let-418(n3636); lin-15A(n767)	0 (77)	92 (78)	Ste
let-418(n3719); lin-15A(n767)	0 (101)	100 (60)	Ste
lin-9(n3631); lin-15A(n767)	100 (42)	100 (72)	Ste
lin-9(n3675); lin-15A(n767)	43 (166)	100 (105)	
lin-9(n3767); lin-15A(n767)	100 (67)	100 (56)	Ste
lin-13(n3642); lin-15A(n767)	3 (60)	100 (63)	Ste
lin-13(n3673); lin-15A(n767)	61 (145)	97 (129)	
lin-13(n3674); lin-15A(n767)	78 (131)	100 (191)	hs Ste
lin-13(n3726); lin-15A(n767)	31 (225)	99 (149)	hs Ste
lin-15B(n3436) lin-15A(n767)	100 (193)	100 (212)	
lin-15B(n3676) lin-15A(n767)	18 (167)	72 (130)	
lin-15B(n3677) lin-15A(n767)	99 (111)	100 (122)	
lin-15B(n3711) lin-15A(n767)	100 (186)	100 (156)	
lin-15B(n3760) lin-15A(n767)	32 (171)	100 (150)	
lin-15B(n3762) lin-15A(n767)	63 (113)	97 (116)	
lin-15B(n3764) lin-15A(n767)	96 (232)	100 (199)	
lin-15B(n3766) lin-15A(n767)	55 (132)	100 (173)	
lin-15B(n3768) lin-15A(n767)	80 (159)	100 (302)	
lin-15B(n3772) lin-15A(n767)	100 (220)	100 (191)	
lin-35(n3438); lin-15A(n767)	100 (153)	100 (126)	Partial Ste at 20°, Rup
lin-35(n3763); lin-15A(n767)	100 (108)	100 (160)	Partial Ste at 20°, Rup
lin-36(n3671); lin-15A(n767)	65 (191)	100 (151)	
lin-36(n3672); lin-15A(n767)	98 (198)	100 (178)	
lin-36(n3765); lin-15A(n767)	0 (184)	37 (202)	
lin-52(n3718); lin-15A(n767)[b]	100 (41)	100 (82)	Ste
lin-53(n3448); lin-15A(n767)	67 (130)	100 (211)	Partial Ste at 20°
lin-53(n3521); lin-15A(n767)	100 (34)	100 (125)	Partial Ste at 20°
lin-53(n3622); lin-15A(n767)	85 (61)	100 (66)	Ste
lin-53(n3623); lin-15A(n767)	24 (55)	100 (51)	Ste
lin-65(n3441); lin-15A(n767)	80 (165)	99 (195)	
lin-65(n3541); lin-15A(n767)	79 (242)	98 (137)	
lin-65(n3543); lin-15A(n767)	85 (177)	100 (121)	
lin(n3628); lin-15A(n767)	3 (103)	84 (188)	
lin(n3542) lin-15A(n767)	0 (127)	35 (218)	

(*continued*)

TABLE 1

(Continued)

Genotype	% Muv (*n*) 15°	% Muv (*n*) 20°	Additional abnormalities
mep-1(n3680); lin-15A(n767)	5 (122)	97 (105)	hs Ste
mep-1(n3702); lin-15A(n767)	30 (61)	100 (141)	Ste
mep-1(n3703); lin-15A(n767)	25 (72)	100 (107)	Ste
mys-1(n3681); lin-15A(n767)[c]	0 (214)	72 (192)	
sli-1(n3538) lin-15A(n767)	4 (138)	90 (173)	
sli-1(n3544) lin-15A(n767)	5 (153)	80 (265)	cs embryonic lethality
sli-1(n3683) lin-15A(n767)	5 (80)	88 (148)	cs embryonic lethality
trr-1(n3630); lin-15A(n767)[c]	3 (131)	85 (212)	Ste, Gro
trr-1(n3637); lin-15A(n767)[c]	1 (92)	80 (200)	Ste, Gro
trr-1(n3704); lin-15A(n767)[c]	3 (96)	79 (244)	Ste, Gro
trr-1(n3708); lin-15A(n767)[c]	2 (151)	84 (228)	Ste, Gro
trr-1(n3709); lin-15A(n767)[c]	1 (97)	77 (154)	Ste, Gro
trr-1(n3712); lin-15A(n767)[c]	6 (121)	77 (192)	Ste, Gro

The penetrance of the Muv phenotype was determined after synMuv mutant strains grew at the indicated temperature for two or more generations. For most strains for which a fully penetrant sterile phenotype was associated with the Muv phenotype, we scored the penetrance of the Muv phenotype by examining sterile progeny of heterozygous mutant parents. For *trr-1* mutant strains, we scored the penetrance of the Muv phenotype by examining non-Gfp progeny of *trr-1/mIn1[dpy-10(e128)mIs14]; lin-15A(n767)* heterozygous parents. All strains were backcrossed to *lin-15A(n767)* twice prior to phenotypic characterization. In addition to the phenotypes described above, many of the strains exhibited heat-sensitive inviability as a consequence of rupture and/or general sickness. Ste, sterile; Gro, growth rate abnormal; Rup, rupture at the vulva; cs, cold sensitive; hs, heat sensitive. The characterization of some of these strains was previously described by:

[a] Ceol and Horvitz (2001),

[b] Thomas *et al.* (2003),

[c] Ceol and Horvitz (2004).

know whether *lin(n3542)* is a synMuv mutation or whether it causes a Muv phenotype on its own.] We used multifactor crosses (Table 2) and deficiency heterozygotes (Table 3) to map these new synMuv genes on their respective linkage groups. While our studies were in progress, *mep-1* and *lin-65* were independently identified and reported to have a loss-of-function synMuv phenotype (Unhavaithaya *et al.* 2002; Poulin *et al.* 2005). Our detailed characterization of the class C synMuv genes *mys-1* and *trr-1* is presented elsewhere (Ceol and Horvitz 2004). We separated *lin-65*, *lin(n3628)*, and *mep-1* mutations from the parental *lin-15A(n767)* mutation and found that these mutations alone do not cause extra vulval cells to be produced (Table 4). Thus, these mutations synergize with *lin-15A(n767)* and are synMuv mutations.

Interactions with other synMuv mutations: Since mutations affecting *lin-65*, *lin(n3628)*, *mep-1*, *gap-1*, *sli-1*, and *ark-1* interact synthetically with a class A synMuv mutation, *lin-15A(n767)*, these genes may be either class B or class C synMuv genes or they may define a new synMuv gene class that shares some but not all properties with class B or class C genes. To distinguish between these possiblities, we built double-mutant strains and measured synthetic interactions with *lin-65*, *lin(n3628)*, *mep-1*, *gap-1*, *sli-1*, and *ark-1* mutations. We used the strongest available mutation for each of these genes in these strain constructions. *ga133* rather than *gap-1(n3535)* was used as the *gap-1* mutation, because *ga133* is a deletion and is considered a null mutation (Hajnal *et al.* 1997). For the sake of brevity, *gap-1(ga133)* is referred to as a "new" synMuv mutation hereafter. We quantified synthetic interactions by directly examining the fates of individual P(3–8).p cells (see materials and methods). In wild-type animals three cells invariably adopt vulval fates, whereas in Muv mutants more than three cells adopt vulval fates.

We first measured synthetic interactions with the class A mutation *lin-38(n751)* and the class B mutations *lin-15B(n744)* and *lin-35(n745)* (Table 4). The new synMuv mutations interacted synthetically not only with *lin-15A (n767)* but also with *lin-38(n751)*, suggesting a general redundancy with the class A synMuv genes. With *lin-15B(n744)* and *lin-35(n745)* the new mutations showed weak to no synthetic interaction.

We also investigated whether the new mutations interacted synthetically with the class C mutation *trr-1(n3712)* (Table 5). In *trr-1(n3712)* single mutants, P8.p adopts a vulval cell fate at a low but detectable penetrance (Ceol and Horvitz 2004). We monitored synthetic interactions with *trr-1(n3712)* for P(3–8).p but report synthetic effects only for P8.p, as this cell is particularly sensitive to cell-fate transformation. *lin-65(n3441)*, *mep-1(n3703)*, *gap-1(ga133)*, and *sli-1(n3538)* but not *lin(n3628)* and *ark-1(n3701)* showed a strong synthetic interaction with *trr-1(n3712)*. In further tests, *ark-1(n3701)* but not *lin(n3628)* interacted synthetically

TABLE 2

Three- and four-factor crosses

Gene	Genotype of heterozygote	Phenotype of selected recombinants	Genotype of selected recombinants (with respect to unselected markers)
lin-65	*+ lin-65 +/bli-3 + lin-17; lin-15A(n767)*	Lin-17	9/19 *lin-65/+*
	bli-3 + lin-65/+ spe-15 +; lin-15A(n767)	Muv	10/18 *spe-15/+*
	+ lin-65 lin-17/spe-15 + +; lin-15A(n767)	Lin-17	11/11 *spe-15/+*
	bli-3 + + + lin-65 +/+ Y73E7.2 Y71G12B.2	Muv	4/30 *Y73E7.2/+*
	Y71G12B.17 + Y71G12B.18; lin-15A(n767)	Muv	2/30 *Y71G12B.2/+*
		Muv	1/30 *Y71G12B.17/+*
		Muv	0/30 *Y71G12B.18/+*
	+ lin-65 + + + lin-17/Y71G12B.17 + Y71G12B.18	Lin-17	17/23 *M01D7.2/+*
	Y71G12B.27 M01D7.2 +; lin-15A(n767)	Lin-17	18/23 *Y71G12B.27/+*
		Lin-17	21/23 *Y71G12B.18/+*
		Lin-17	23/23 *Y71G12B.17/+*
lin(n3542)	*+ + lin(n3542) lin-15A(n767)/unc-10 dpy-6 + lin-15A(n767)*	Unc	8/8 *lin(n3542)/+*
	+ lin(n3542) + lin-15A(n767)/dpy-6 + unc-9 lin-15A(n767)	Unc	4/40 *lin(n3542)/+*
lin(n3628)	*lin(n3628) + +/+ dpy-5 unc-13; lin-15A(n767)*	Dpy	0/6 *lin(n3628)/+*
		Unc	6/6 *lin(n3628)/+*
	+ lin(n3628) +/unc-11 + dpy-5; lin-15A(n767)	Unc	1/11 *lin(n3628)/+*
		Dpy	5/11 *lin(n3628)/+*
	unc-11 + + lin(n3628)/+ unc-73 lin-44 +; lin-15A(n767)	Muv	3/9 *unc-73 lin-44/++*
	+ + lin(n3628) dpy-5/unc-73 lin-44 + +; lin-15A(n767)	Muv	0/21 *unc-73 lin-44/++*
	lin(n3628) + dpy-5/+ unc-38 +; lin-15A(n767)	Muv	3/7 *unc-38/+*
	unc-11 lin(n3628) +/+ + unc-38; lin-15A(n767)	Muv	0/9 *unc-38/+*
mep-1	*+ mep-1 +/unc-5 + dpy-20; lin-15A(n767)*	Unc	56/57 *mep-1/+*
		Dpy	2/61 *mep-1/+*
	mep-1 + +/+ dpy-20 unc-30; lin-15A(n767)	Dpy	0/51 *mep-1/+*
		Unc	58/58 *mep-1/+*
	+ + mep-1 +/unc-24 mec-3 + dpy-20; lin-15A(n767)	Unc Mec	10/12 *mep-1/+*
		Unc	17/17 *mep-1/+*
		Mec Dpy	0/8 *mep-1/+*
		Dpy	2/8 *mep-1/+*
	+ mep-1 dpy-20 +/lin-3 + + unc-22; lin-15A(n767)	Dpy	5/5 *lin-3/+*
		Vul	3/10 *mep-1/+*
	+ + mep-1+/mec-3 sem-3 + dpy-20; lin-15A(n767)	Mec	17/17 *mep-1/+*
		Dpy	6/13 *mep-1/+*
mys-1	*+ mys-1 +/unc-46 + dpy-11; lin-15A*	Unc	3/7 *mys-1/+*
		Dpy	7/11 *mys-1/+*
trr-1	*+ rol-6 + trr-1/dpy-10 + unc-4 +; lin-15A(n767)*	Rol	3/14 *unc-4/+*
		Dpy	3/3 *trr-1/+*
		Unc	0/8 *trr-1/+*
	+ trr-1 +/dpy-10 + rol-1; lin-15A(n767)	Rol	9/20 *trr-1/+*
	+ + trr-1/dpy-10 unc-53 +; lin-15A(n767)	Unc	0/17 *trr-1/+*
	+ trr-1 +/unc-53 + rol-1; lin-15A(n767)	Unc	7/10 *trr-1/+*
		Rol	7/10 *trr-1/+*
	+ trr-1 + rol-1/unc-4 + mex-1 +; lin-15A(n767)	Rol	12/14 *mex-1/+*

Three- and four-factor crosses were performed using standard methods (Brenner 1974). We mapped *lin-65* using the *Y73E7.2*, *Y71G12B.2*, *Y71G12B.17*, *Y71G12B.18*, *Y71G12B.27*, *M01D7.2* DNA sequence polymorphisms present in the CB4856 strain.

with the class C mutation *mys-1(n3681)*: *ark-1(n3701); mys-1(n3681)* double mutants had a strong synthetic P8.p vulval fate defect (80%, $n = 41$) as compared to *ark-1(n3701)* (0%, $n = 33$) and *mys-1(n3681)* (8.3%, $n = 36$) single mutants, whereas the P8.p vulval-fate defect of *lin(n3628); mys-1(n3681)* (6.7%, $n = 30$) double mutants was low, like that of *lin(n3628)* (0%, $n = 37$) and *mys-1(n3681)* single mutants. Why *ark-1(n3701)* interacted with one class C mutation but not another is unclear. It is possible that the synthetic interaction with *ark-1(n3701)* is sensitive to maternally provided levels of class C synMuv activity and *mys-1(n3681)*, which can be maintained in homozygous strains, provided less maternal activity than did *trr-1(n3712)*, which because of its recessive sterility requires that homozygotes be generated from heterozygous parents.

Most of the new mutations interacted synthetically with class A and class C but not with class B mutations,

TABLE 3

Deficiency heterozygote mapping

Gene	Genotype of heterozygote	Phenotype of heterozygote
mep-1	*mep-1/sDf63 unc-31; lin-15A(n767)/+*	Pvl Ste
	mep-1/sDf62 unc-31; lin-15A(n767)/+	Pvl Ste
	mep-1/sDf10; lin-15A(n767)/+	WT
trr-1	*rol-6 trr-1/mnDf57; lin-15A(n767)*	WT
	rol-6 trr-1/unc-4 mnDf90; lin-15A(n767)	WT
	rol-6 trr-1/mnDf29; lin-15A(n767)	WT
	trr-1/unc-4 mnDf87; lin-15A(n767)	Muv

Deficiency heterozygotes were constructed as described in MATERIALS AND METHODS. WT, wild type; Pvl, protruding vulva; Ste, sterile.

which indicates that these new mutations are neither class A nor class C mutations. The synthetic interaction of *lin(n3628)* with class A but not with class B or class C mutations is unusual and is discussed below.

Suppression of *let-23* mutations: Are *lin-65*, *lin(n3628)*, *mep-1*, *gap-1*, *sli-1*, and *ark-1* class B synMuv genes? Neither in combination with class A mutations (FERGUSON *et al.* 1987; LU and HORVITZ 1998; THOMAS and HORVITZ 1999; CEOL and HORVITZ 2001) nor on their own (Table 6) do class B mutations suppress the Vul phenotype caused by strong loss-of-function *let-23* receptor tyrosine kinase mutations. However, previous studies showed that *gap-1* or *sli-1* mutations alone can suppress the *let-23* Vul phenotype (JONGEWARD *et al.* 1995; HAJNAL *et al.* 1997). Together these findings distinguish *gap-1* and *sli-1* from class B synMuv genes and indicate that *let-23* suppression may be used as a criterion in classifying synMuv mutations. We found that mutations affecting *lin-65*, *lin(n3628)*, *mep-1*, and *ark-1* did not suppress the *let-23* Vul phenotype (Table 6), suggesting that these genes are not in the same class as *gap-1* and *sli-1*.

Interactions with *ark-1*, *gap-1*, and *sli-1* mutations: *gap-1* and *sli-1* mutations interact synthetically to produce extra vulval cells (Table 7). Furthermore, an *ark-1* mutation interacts synthetically with these *gap-1* and *sli-1* mutations, suggesting that all three genes act in parallel in regulating vulval cell fates. Similar synergism of an *ark-1* mutation with *gap-1* and *sli-1* mutations was observed previously (HOPPER *et al.* 2000). By contrast, we observed that the class B synMuv mutations *lin-15B(n744)* and *lin-35(n745)* did not interact synthetically with *gap-1* or *sli-1* mutations (Table 4). This lack of synergism is likely not the result of using weak alleles, as the *lin-15B(n744)*, *lin-35(n745)*, *gap-1(ga133)*, and *sli-1(n3538)* mutations used in these studies are strong loss-of-function, and possibly null, mutations of their corresponding genes. These results distinguish *ark-1* from the class B genes *lin-15B* and *lin-35* Rb and suggest that these class B genes do not act with *ark-1* in antagonizing Ras pathway activity. *lin-65*, *lin(n3628)*, and *mep-1* mutations also did not interact synthetically with *gap-1(ga133)* or *sli-1(n3538)* (Table 7), revealing a further similarity between *lin-65*, *lin(n3628)*, and *mep-1* mutations and *lin-15B* and *lin-35* Rb class B synMuv mutations.

Molecular identification of *lin-65*: We mapped the synMuv gene *lin-65* to a small interval between the *C. elegans* strain CB4856 polymorphisms *Y71G12B.17* and *Y71G12B.18* (Figure 1A). This interval contains four complete predicted genes, one of which is a micro RNA gene, and portions of three other genes, two of which overlap (*C. elegans* SEQUENCING CONSORTIUM 1998). We performed RNA-mediated interference (RNAi) to determine if inactivation of any of the three complete, protein-encoding genes would result in a synMuv phenotype. RNAi of Y71G12B.9 caused a Muv phenotype in a *lin-15A(n767)* but not in a wild-type or *lin-15B(n744)* background (data not shown). POULIN *et al.* (2005) independently found that RNAi of Y71G12B.9 caused a synMuv phenotype. We obtained six cDNAs (kindly provided by Yuji Kohara and co-workers) and compared the sequences of these clones with genomic sequence to determine a gene structure for Y71G12B.9 (Figure 1B). One clone had an SL1 and two had an SL2 splice-leader sequence. The presence of an SL2 splice leader suggests that Y71G12B.9 is a downstream gene in an operon (ZORIO *et al.* 1994). The predicted initiator methionine codon of the SL2-spliced Y71G12B.9 cDNAs lies just downstream of the *trans*-splice site. The open reading frame beginning with this initiator methionine encodes a 728-amino-acid protein (Figure 2). The SL1 *trans*-splice site is downstream from that of SL2, and the single SL1-spliced cDNA lacks the initiator methionine corresponding to the 728-amino-acid predicted protein. The open reading frames defined by the first three potential initiator methionine codons of the SL1-spliced cDNA are all short (≤16 codons). If the fourth potential initiator methionine codon were used, a 691-amino-acid protein lacking the first 37 amino acids of the 728-amino-acid protein described above would be synthesized. Expression under the control of the *C. elegans* heat-shock promoters of a cDNA predicted to encode the 728-amino-acid protein rescued the Muv phenotype of *lin-65* mutants: two transgenic lines of *lin-65(n3441); lin-15A(n767)* mutants containing P_{hs}:*lin-65* transgenes

TABLE 4

Interactions of new mutations with class A and class B synMuv mutations

		Single mutant		Double mutant with class A				Double mutant with class B			
				lin-15A(n767)		*lin-38 (n751)*		*lin-15B(n744)*		*lin-35(n745)*	
		% >3 vulval fates (*n*)	Ave. no. vulval fates (±SE)	% >3 vulval fates (*n*)	Ave. no. vulval fates (±SE)	% >3 vulval fates (*n*)	Ave. no. vulval fates (±SE)	% >3 vulval fates (*n*)	Ave. no. vulval fates (±SE)	% >3 vulval fates (*n*)	Ave. no. vulval fates (±SE)
New mutation	*lin-65(n3441)*	0 (35)	3.0 (±0)	100 (36)	5.9 (±0.04)	97 (37)	5.3 (±0.13)	4.3 (23)	3.02 (±0.02)	ND	ND
	lin(n3628)	0 (37)	3.0 (±0)	71 (41)	3.9 (±0.14)	92 (24)	4.4 (±0.15)	2.7 (37)	3.01 (±0.01)	0 (31)	3.0 (±0)
	mep-1(n3703)	2.5 (40)	3.01 (±0.01)	100 (29)	6.0 (±0.19)	100 (36)	5.9 (±0.29)	0 (21)	3.0 (±0)	0 (25)	3.0 (±0)
	ark-1(n3701)	0 (33)	3.0 (±0)	77 (30)	4.5 (±0.20)	56 (34)	3.8 (±0.14)	7.8 (26)	3.06 (±0.04)	7.4 (27)	3.07 (±0.05)
	gap-1(ga133)	3.1 (32)	3.02 (±0.02)	58 (38)	3.6 (±0.11)	76 (37)	4.4 (±0.17)	0 (29)	3.0 (±0)	0 (30)	3.0 (±0)
	sli-1(n3538)	0 (25)	3.0 (±0)	93 (28)	4.6 (±0.16)	30 (27)	3.3 (±0.11)	0 (36)	3.0 (±0)	4.5 (22)	3.02 (±0.02)
Class A	*lin-15A(n767)*	0 (24)[a]	3.0 (±0)[a]			—[c]	—[c]	ND	ND	—[c]	—[c]
	lin-38 (n751)	0 (27)[a]	3.0 (±0)[a]	0 (32)	3.0 (±0)			—[c]	—[c]	—[c]	—[c]
Class B	*lin-15B(n744)*	0 (20)	3.0 (±0)	ND	ND	100 (33)	6.0 (±0)			—[c]	—[c]
	lin-35(n745)	0 (48)	3.0 (±0)	100 (22)	6.0 (±0)	100 (27)	6.0 (±0)	0 (26)	3.0 (±0)		
Class C	*mys-1(n3681)*	8.3 (36)[b]	3.06 (±0.03)[b]	100 (26)[b]	5.04 (±0.14)[b]	91 (45)[b]	4.40 (±0.13)[b]	46 (37)	3.38 (±0.08)	ND	ND
	trr-1(n3712)	13 (89)[a]	3.10 (±0.03)[a]	74 (54)[a]	4.07 (±0.12)[a]	79 (14)[a]	4.14 (±0.23)[a]	50 (38)	3.38 (±0.07)	63 (41)	3.43 (±0.06)

New synMuv mutations were separated from *lin-15A(n767)*, and double-mutant strains were constructed as described in MATERIALS AND METHODS. Because these mutations cause recessive sterility, *mep-1(n3703)* and *trr-1(n3712)* homozygotes were derived from heterozygous parents. *mep-1(n3703)* homozygotes were recognized as the non-Unc progeny of *mep-1(n3703)/nT1 n754* heterozygous parents or the non-Gfp progeny of *mep-1(n3703)/nT1[qIs51]* heterozygous parents. *trr-1(n3712)* homozygotes were recognized as the non-Gfp progeny of *trr-1(n3712)/mIn1[dpy-10(e128) mIs14]* heterozygous parents. The *lin(n3628) lin-35* strain was marked with *unc-13*. ND, not determined.

[a] These data are from Table 1 of CEOL and HORVITZ (2004).

[b] These data are from Table 3 of CEOL and HORVITZ (2004).

[c] These data are found elsewhere in this table.

TABLE 5

Interactions of new mutations with the class C synMuv mutation *trr-1(n3712)*

		% animals with P8.p vulval fate	
		trr-1(+)	*trr-1(n3712)*
	+	0 (many)	13 (89)[a]
New mutation	*lin-65(n3441)*	0 (35)	45 (31)
	lin(n3628)	0 (37)	4.2 (24)
	mep-1(n3703)	2.5 (40)	Let[b]
	ark-1(n3701)	0 (33)	13 (24)
	gap-1(ga133)	3.1 (32)	37 (38)
	sli-1(n3538)	0 (25)	32 (37)
Class A	*lin-15A(n767)*	0 (24)	28 (54)
	lin-38(n751)	0 (27)	36 (14)
Class B	*lin-15B(n744)*	0 (20)[a]	50 (38)[a]
	lin-35(n745)	0 (48)[a]	64 (41)[a]

Double-mutant strains were constructed as described in MATERIALS AND METHODS. *mep-1(n3703)* homozygotes were recognized as the non-Unc progeny of *mep-1(n3703)/nT1 n754* heterozygous parents or the sterile progeny of *mep-1(n3703)/dpy-20(e1282) unc-30(e191)* heterozygous parents. *trr-1(n3712)* homozygotes were recognized as the non-Gfp progeny of *trr-1(n3712)/mIn1[dpy-10(e128) mIs14]* heterozygous parents.

[a] These data are from Table 1 of CEOL and HORVITZ (2004).

[b] We interpret this synthetic lethality as indicating redundancy between *mep-1* and *trr-1*.

were 0% ($n = 73$) and 2.0% ($n = 49$) non-Muv without heat shock but were 71% ($n = 68$) and 67% ($n = 30$) non-Muv, respectively, following heat-shock treatment.

We determined the sequence of Y71G12B.9 in *lin-65(n3441)*, *lin-65(n3541)*, and *lin-65(n3543)* mutants. *lin-65(n3441)* and *lin-65(n3541)* contain identical nonsense mutations predicted to truncate the Y71G12B.9 protein after 533 of the 728 amino acids. It is unlikely that *lin-65(n3441)* and *lin-65(n3541)* were caused by the same mutational event, since they were isolated from independently mutagenized and screened P_0 animals. *lin-65(n3543)* contains a missense mutation that changes a polar serine residue to a nonpolar leucine (S720L). The map position, RNAi phenocopy, and cDNA rescue data as well as the mutant allele sequences indicate that Y71G12B.9 is *lin-65*.

The 728-amino-acid LIN-65 protein is rich in acidic amino acids (Figure 2). Over 7 and 10% of the total number of amino acids are aspartates and glutamates, respectively, and these acidic amino acids are found both in clusters and dispersed throughout LIN-65. BLAST searches (ALTSCHUL *et al.* 1990) with LIN-65 identified proteins from mammalian and other species that are similarly acid rich. Because the similarity between LIN-65 and these proteins is primarily limited to acidic residues and not to specific protein domains (data not shown), it is difficult to predict whether these proteins are functional orthologs of LIN-65. As described above, mutations in *lin-65* and *lin-35* Rb show similar genetic interactions, suggesting that *lin-65* is a class B synMuv gene that acts in the *lin-35* Rb pathway. Protein complexes purified from Drosophila extracts and analogous to a class B synMuv complex (M. M. HARRISON and H. R. HORVITZ, unpublished observations) have not been reported to contain LIN-65-like proteins (KORENJAK *et al.* 2004; LEWIS *et al.* 2004). It is possible that LIN-65 and LIN-65 orthologs act upstream of class B synMuv and analogous complexes to promote complex activity or act downstream as effectors of these complexes.

Sequences of synMuv mutations: We determined DNA sequences of 41 mutant synMuv genes identified in our screen; 4 of these mutant genes had two distinct mutations (Table 8). The 41 include all of the *dpl-1*, *efl-1*, *let-418*, *lin-9*, *lin-13*, *lin-36*, *lin-52*, *lin-53*, *lin-65*, *mep-1*, *mys-1*, *sli-1*, and *trr-1* alleles and one of two *lin-35* alleles identified in our screen. Forty of 45 mutations are GC-to-AT transitions, which are characteristic of EMS mutagenesis (ANDERSON 1995). Many of these mutations are predicted to truncate the corresponding synMuv proteins. The truncations predicted by *efl-1(n3639)*, *let-418(n3719)*, *lin-52(n3718)*, and *trr-1(n3704)* are particularly severe, and the synMuv and sterile abnormalities caused by these mutations likely represent the null phenotypes of these genes. In addition, we found missense mutations that disrupt predicted functional domains of synMuv proteins. For example, *n3536*, *n3626*, *n3629*, and one of the two mutations of *n3636* affect the ATPase/helicase domain of LET-418. LET-418 is a member of the Mi-2 family of ATP-dependent chromatin remodeling enzymes (SOLARI and AHRINGER 2000; VON ZELEWSKY *et al.* 2000), and the LET-418 missense mutations suggest that LET-418 function is dependent on ATP hydrolysis. At least one mutation affecting the LIN-13 protein, *n3642*, is predicted to disrupt a canonical zinc-finger motif. This missense mutation, along with those isolated previously (THOMAS *et al.* 2003), indicates that at least some of the 24 LIN-13 zinc fingers are important for LIN-13 synMuv activity. Missense mutations affecting other synMuv proteins are not as easily linked to the disruption of predicted functional domains. These mutations may provide useful starting points for identifying functional motifs within synMuv proteins that are not predicted by sequence comparisons.

DISCUSSION

Frequency of mutant isolation: The rate at which we isolated synMuv mutations was much higher than that observed in previous screens. Considering screens that were conducted in class A synMuv mutant backgrounds, we recovered one synMuv mutation per 109 haploid genomes screened as compared with one per 750

TABLE 6

Suppression of the *let-23* vulvaless phenotype

		Ave. no. vulval fates (±SE, *n*)	
		let-23(+)	*let-23(sy97)*
	+	3.0 (many)	0 (±0, 36)
New mutation	*lin-65(n3441)*	3.0 (±0, 35)[a]	0 (±0, 30)
	lin(n3628)	3.0 (±0, 37)[a]	Let[d]
	mep-1(n3703)	3.01 (±0.01, 40)[a]	Let[d]
	ark-1(n3701)	3.0 (±0, 33)[a]	0.10 (±0.05, 34)
	gap-1(ga133)	3.02 (±0.02, 32)[a]	3.0 (±0, 26)
	sli-1(n3538)	3.0 (±0, 25)[a]	3.0 (±0, 31)
Class A	*lin-15A(n767)*	3.0 (±0, 24)[b]	0 (±0, 21)
	lin-38(n751)	3.0 (±0, 27)[b]	ND
Class B	*lin-15B(n744)*	3.0 (±0, 20)[a]	0.23 (±0.08, 26)
	lin-35(n745)	3.0 (±0, 48)[a]	0.20 (±0.06, 38)
Class C	*mys-1(n3681)*	3.06 (±0.03, 36)[c]	1.47 (±0.15, 31)
	trr-1(n3712)	3.10 (±0.03, 89)[b]	0.28 (±0.07, 46)

mep-1(n3703) homozygotes were recognized as the non-Unc progeny of *mep-1(n3703)/nT1 n754* heterozygous parents or the sterile progeny of *mep-1(n3703)/dpy-20(e1282) unc-30(e191)* heterozygous parents. *trr-1(n3712)* homozygotes were recognized as the non-Gfp progeny of *trr-1(n3712) / mIn1[dpy-10(e128) mIs14]* heterozygous parents. *let-23(sy97)* was marked with *unc-4(e120)*, and *let-23(sy97)* homozygotes were recognized as the Unc non-Gfp progeny of *let-23(sy97) unc-4(e120)/mIn1[dpy-10(e128) mIs14]* heterozygous parents. ND, not determined because of linkage of these mutations.

[a] These data are from Table 1.

[b] These data are from Table 1 of Ceol and Horvitz (2004).

[c] These data are from Table 3 of Ceol and Horvitz (2004).

[d] Because of the lethality of these animals, we measured the abilities of *lin(n3628)* and *mep-1(n3703)* to suppress the Vul phenotype caused by *sy10*, a *let-23* allele that is weaker than *sy97*. *lin(n3628)* and *mep-1(n3703)* were unable to suppress the Vul phenotype of *let-23(sy10)*: *lin(n3628); let-23(sy10)* double mutants averaged 0.11 vulval fates ($n = 27$), *let-23(sy10); mep-1(n3703)* double mutants averaged 0.06 vulval fates ($n = 24$), and *let-23(sy10)* single mutants averaged 0.14 vulval fates ($n = 21$).

(Ferguson and Horvitz 1989), one per 400 (Thomas *et al.* 2003), and one per 667 (Thomas *et al.* 2003) in previous screens. We believe the reasons for this difference are threefold. First, our screen design allowed the isolation of synMuv mutations that also caused sterility. Numerous sterile synMuv mutants had been observed in previous screens, but in general the mutations responsible were not recovered. Second, our parental strain carried a strong class A mutation, *lin-15A(n767)*. The penetrance of the Muv phenotype of a synMuv strain is dependent on the combined strengths of the individual synMuv mutations (C. J. Ceol and

TABLE 7

Interactions of new mutations with *gap-1* and *sli-1* mutations

		Double mutant with *gap-1(ga133)*		Double mutant with *sli-1(n3538)*	
		% >3 vulval fates (*n*)	Ave. no. vulval fates (±SE)	% >3 vulval fates (*n*)	Ave. no. vulval fates (±SE)
New mutation	*lin-65(n3441)*	0 (31)	3.0 (±0)	0 (34)	3.0 (±0)
	lin(n3628)	6.1 (33)	3.05 (±0.03)	0 (36)	3.0 (±0)
	mep-1(n3703)	8.3 (36)	3.07 (±0.04)	5.6 (36)	3.03 (±0.02)
	ark-1(n3701)	83 (40)	4.18 (±0.14)	48 (29)	3.48 (±0.11)
	gap-1(ga133)			46 (35)	3.51 (±0.11)

Double-mutant strains were constructed as described in materials and methods. *mep-1(n3703)* homozygotes were recognized as the sterile progeny of *mep-1(n3703)/dpy-20(e1282) unc-30(e191)* heterozygous parents. *trr-1(n3712)* homozygotes were recognized as the non-Gfp progeny of *trr-1(n3712)/mIn1[dpy-10(e128) mIs14]* heterozygous parents.

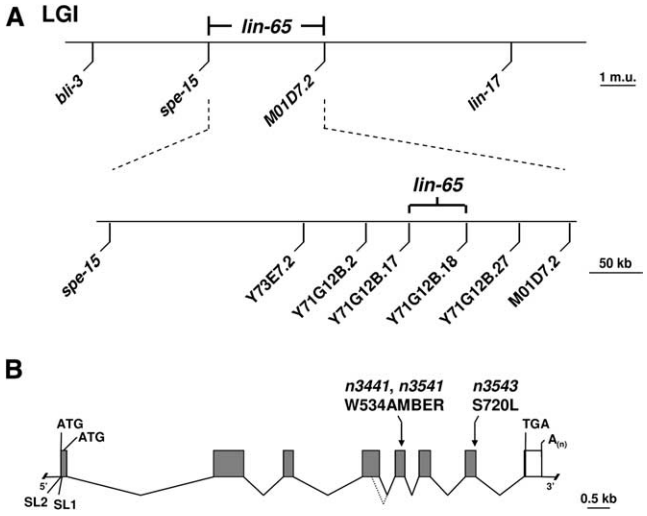

FIGURE 1.—Molecular cloning of *lin-65*. (A) The genetic map location of *lin-65* on linkage group I (top) and the physical map interval between the *C. elegans* strain CB4856 polymorphisms *Y71G12B.17* and *Y71G12B.18* and including *lin-65* (bottom). (B) *lin-65* gene structure as derived from cDNA and genomic sequences. Shaded boxes indicate coding sequence and an open box indicates the 3′-untranslated region (*lin-65* transcripts also contain a 5′-untranslated region that is too small to be viewed in this representation). Predicted translation initiation and termination codons and the poly(A) tail are shown. Arrows above indicate the positions of the *lin-65(n3441)*, *lin-65(n3541)*, and *lin-65(n3543)* mutations. The fourth exon of the cDNA yk1279h11 is smaller than that of the other five *lin-65* cDNAs (the end of the yk1279h11 fourth exon is indicated by a dashed line). The use of an alternative splice donor may have created this shorter fourth exon. However, if the end of the yk1279h11 fourth exon were the site of alternative splicing, a CA and not the typical GT splice donor would have been used. In addition, the end of the yk1279h11-specific fourth exon and the beginning of the fifth exon encode multiple glutamine residues and are highly similar in DNA sequence (see Figure 2). The intervening sequence between two regions of highly similar sequence can be lost because of recombination in bacteria (ROBINETT *et al.* 1996). For these reasons we speculate that the apparent alternative splice site at the end of the fourth exon in yk1279h11 may be artifactual and have resulted from an error during the generation or maintenance of this cDNA clone. In support of this possibility: (1) We failed to amplify a shorter-than-wild-type yk1279h11 product in a high-stringency RT–PCR using oligonucleotide primers that flank the putative alternative splice junction, and (2) we failed to amplify any RT–PCR products when an oligonucleotide spanning the putative yk1279h11 alternative splice junction was used in a PCR.

H. R. HORVITZ, unpublished observations). Therefore, even weak mutations could be identified in a strong synMuv background such as *lin-15A(n767)*. Such weak mutations may not have been recovered in the three previous screens described above, all of which were performed in partial loss-of-function synMuv backgrounds. Third, by screening petri plates with many F_2 progeny derived from a single F_1 animal, we observed many genotypically identical animals for each haploid genome screened. Such screening can efficiently recover partially penetrant synMuv mutations.

Of the 62 mutations described in this study, 24 caused recessive sterility. The 38 mutations that did not cause sterility were recovered at 1 mutation per 178 haploid genomes screened, a frequency higher than that of previous screens. The difference in the rate of recovery of nonsterile mutants is likely a consequence of the second and third differences in screening described above.

Given that the average gene mutates to loss of function at a rate of $\sim 5 \times 10^{-4}$ under the conditions of EMS mutagenesis we used (BRENNER 1974; MENEELY and HERMAN 1979; GREENWALD and HORVITZ 1980), our observed rate of 10^{-2} suggests that ~20 genes can mutate by loss of function to cause a synMuv phenotype in combination with a class A synMuv mutation. Including the genes we identified in this study, a total of 25 such genes have been described to date. Three or fewer alleles of 15 of these genes have been recovered in synMuv screens, indicating that screens for such genes are not saturated.

Different synMuv gene classes likely act in parallel to antagonize *let-60* Ras pathway activity: Class A synMuv mutations synergize with class B mutations but not with other class A mutations, whereas class B synMuv mutations synergize with class A synMuv mutations but not with other class B synMuv mutations. Such genetic behavior led to the hypothesis that the A and B classes of synMuv genes encode components of two functionally redundant pathways that negatively regulate vulval development (FERGUSON and HORVITZ 1989). Consistent with this hypothesis, a subset of class B synMuv gene products has been shown to physically interact and their homologs are known to function together in other organisms (LU and HORVITZ 1998; CEOL and HORVITZ 2001; UNHAVAITHAYA *et al.* 2002; KORENJAK *et al.* 2004; LEWIS *et al.* 2004).

Because we conducted our screen using a class A synMuv background, we anticipated recovering mutations that affected class B synMuv genes. Indeed, 47 of the 62 mutations we isolated affected previously known and newly described class B synMuv genes. However, we discovered that some new mutations define new classes of synMuv genes. synMuv mutations previously were categorized by testing for synergism with class A and class B mutations. From such tests we discovered that some of our new mutations synthetically interacted with both class A and class B mutations; such mutations defined the class C genes *trr-1* and *mys-1* (this study and CEOL and HORVITZ 2004). Other new mutations interacted like class B mutations in these standard tests but were distinguished from class B mutations by additional tests. For example, like class B mutations *sli-1(n3538)* synthetically interacted with class A but not with class B mutations yet, unlike class B mutations synthetically interacted with *ark-1* and *gap-1* and suppressed the *let-23* Vul phenotype. These results led us to adopt two criteria when classifying synMuv mutations: (1) If two

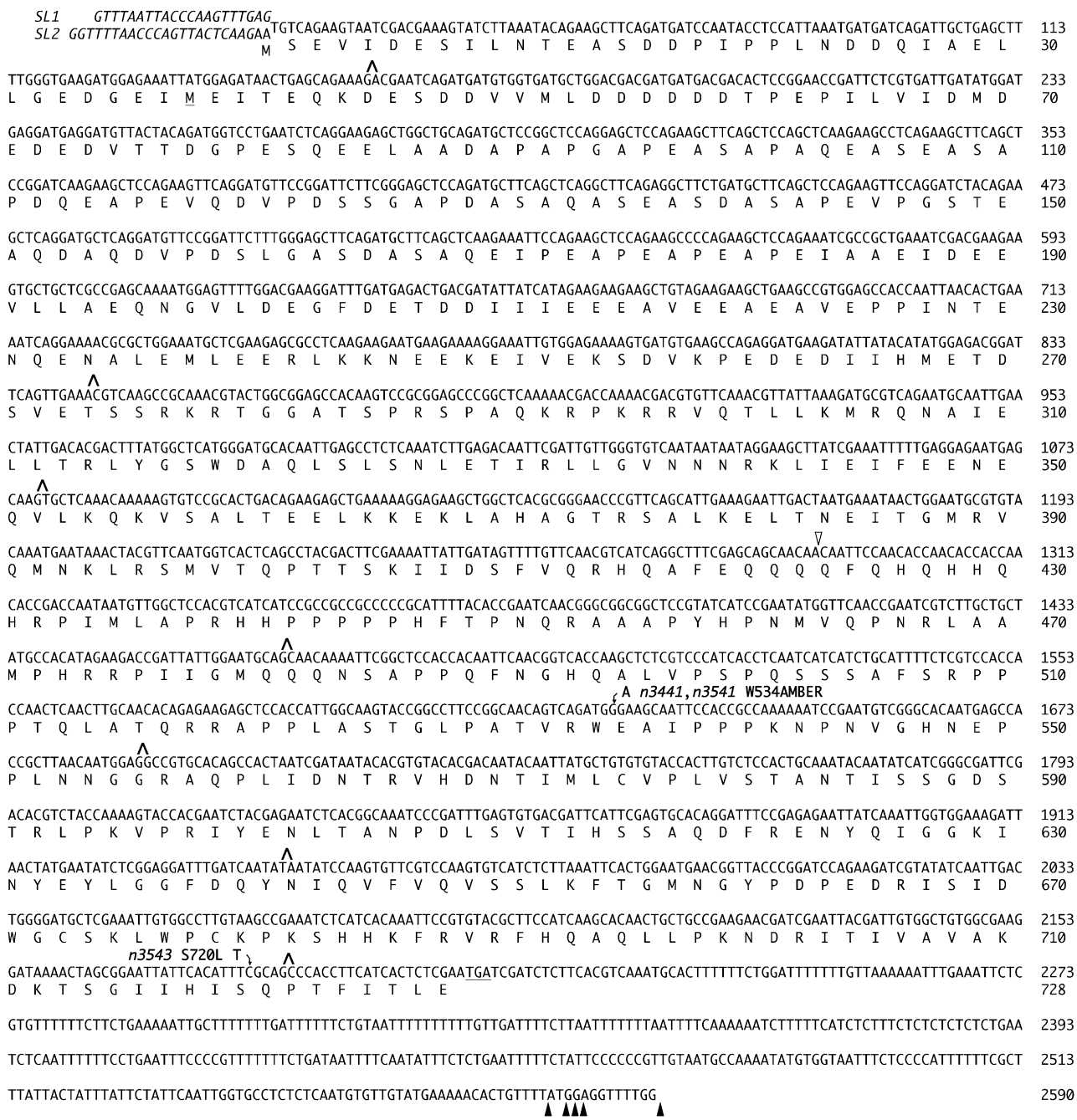

FIGURE 2.—*lin-65* cDNA sequence indicating differences among individual *lin-65* cDNAs. SL1 and SL2 splice-leader sequences are italicized. The SL1 leader, as observed with one cDNA, is spliced two nucleotides downstream of the site at which the SL2 leader is spliced, as observed with two independently derived cDNAs. Intron positions are indicated by carats. The translation termination codon is underlined. Sites of alternative polyadenylation are indicated with solid arrowheads. The predicted LIN-65 protein is shown beneath. The SL2-spliced cDNAs are predicted to encode a 728-amino-acid protein. The SL1-spliced cDNA cannot encode the predicted initiator methionine of the 728-amino-acid protein; it may use the underlined methionine codon to initiate synthesis of a 691-amino-acid protein. The alternatively spliced cDNA yk1279h11 is predicted to encode a protein lacking amino acids 421–481 of the 728-amino-acid protein, although, as described in the Figure 1 legend, the alternative splicing of yk1279h11 is likely to be artifactual. The site at which the putative fourth exon in yk1279h11 ends is indicated with an open arrowhead. This end is juxtaposed to the beginning of the fifth exon to give a CAGCAACAA/CAACAAAAT junction sequence.

mutations synthetically interact to cause a Muv phenotype, then they are in different classes, and (2) if two mutations do not synthetically interact but interact differently with other classes of synMuv mutations or with *let-23*, then they are in different classes. Since we have found that interaction tests with only class A and class B mutations are insufficient to classify some synMuv genes, we suggest that previously described

TABLE 8

Sequences of new mutations of class B and class C synMuv proteins

Protein	Class	No. amino acids	Protein similarities and domains[a]
			A. Features of synMuv proteins
DPL-1	B	598	Similar to DP family transcription factors; contains DNA- and E2F-binding domains.
EFL-1	B	342	Similar to E2F family transcription factors; contains DNA-, DP- and Rb-binding domains.
LET-418	B	1829	Similar to Mi-2 family ATP-dependent chromatin remodeling enzymes; contains chromodomains, PHD finger motifs, and a helicase domain[b]
LIN-9	B	LIN-9L: 644 LIN-9S: 642	Similar to Drosophila Mip130 DNA replication and Aly cell cycle regulators and mammalian proteins of unknown function.
LIN-13	B	2248	24 predicted Zn-finger motifs.
LIN-35	B	961	Similar to Retinoblastoma (pRb) family transcriptional regulators; contains "pocket" interaction domain.
LIN-36	B	962	THAP domain, C/H-rich and Q-rich regions.
LIN-52	B	161	Similar to Drosophila and mammalian proteins of unknown function.
LIN-53	B	417	Similar to Drosophila p55, mammalian RbAp48 subunits of chromatin remodeling, and histone deacetylase complexes; contains WD repeats.
LIN-65	B	728	Acid rich
MEP-1	B	853	Six Zn-finger motifs.
MYS-1	C	458	Similar to MYST family histone acetyltransferases; contains chromodomain and acetyltransferase domain.
SLI-1	*sli-1*	582	Similar to Cbl family ubiquitination-promoting proteins; contains SH2 domain and RING finger motif.
TRR-1	C	4064[c]	Similar to mammalian TRRAP transcriptional regulator.

Mutation	Wild-type sequence	Mutant sequence	Substitution, splice site change, or aberration	Domain affected by missense mutation
			B. Allele sequences	
dpl-1(n3643)[d]	TAT	TAA	Y341ochre	—
	GGC	CGC	G533R	Unknown
efl-1(n3639)[e]	CAA	TAA	Q175ochre	—
let-418(n3536)	CCT	CTT	P675L	Helicase/ATPase
let-418(n3626)	GGT	AGT	G1006S	Helicase/ATPase
let-418(n3629)	TCC	TTC	S925F	Helicase/ATPase
let-418(n3634)	TGG	TAG	W1128amber	—
let-418(n3635)	CAG	TAG	Q1594amber	—
let-418(n3636)	ACT	TCT	T807S	Helicase/ATPase
	TGG	TGA	W1329opal	—
let-418(n3719)	TGG	TAG	W295amber	—
lin-9(n3631)	CAA	TAA	LIN-9L: Q594ochre	—
			LIN-9S: Q592ochre	—
lin-9(n3675)	GAT	AAT	LIN-9L: D305N	Unknown
			LIN-9S: D303N	Unknown
lin-9(n3767)	CAG	TAG	LIN-9L: Q509amber	—
			LIN-9S: Q507amber	—
lin-13(n3642)	CAT	TAT	H832Y	Zn finger
lin-13(n3673)	CAG	TAG	Q1988amber	—
lin-13(n3674)	CGA	TGA	R1250opal	—
lin-13(n3726)	GGA	GAA	G229E	Unknown
lin-35(n3763)[f]	GCA	GTA	A555V	Pocket
	TTG AAA AAG	TTG AAA AAA G	K594 frameshift and truncation after 611 a.a.	—
lin-36(n3671)	CAT	CCT	H284P	C/H-rich region
	GAA	AAA	E424K	Unknown
lin-36(n3672)	CAG	TAG	Q467amber	—
lin-36(n3765)[g]	GCT	GTT	A242V	C/H-rich region
lin-52(n3718)[h]	CAG	TAG	Q31amber	—
lin-53(n3448)	AGT	ATT	S384I	WD repeat
lin-53(n3521)	GAA	AAA	E174K	WD repeat

(*continued*)

TABLE 8

(Continued)

Mutation	Wild-type sequence	Mutant sequence	Substitution, splice site change, or aberration	Domain affected by missense mutation
lin-53(n3622)	AAG/gtatgtgt	AAG/atatgtgt	Exon 1 donor	—
lin-53(n3623)	TGG	TAG	W337amber	—
lin-65(n3441)	TGG	TGA	W534amber	—
lin-65(n3541)	TGG	TGA	W534amber	—
lin-65(n3543)	TCG	TTG	S720L	Unknown
mep-1(n3680)	AGT	AAT	S309N	Unknown
mep-1(n3702)	CAG	TAG	Q706amber	—
mep-1(n3703)	CTT/gtaagttt	CTT/ataagttt	Exon 3 donor	—
mys-1(n3681)[i]	GGA	AGA	G341R	Acetyltransferase
sli-1(n3538)	TCA	TTA	S305L	SH2
sli-1(n3544)	ttttccag/AAA	ttttccaa/AAA	Exon 6 acceptor	—
sli-1(n3683)	ttttttag/GAT	tttttaa/GAT	Exon 4 acceptor	—
trr-1(n3630)[j]	TGG	TAG	W2064amber	—
trr-1(n3637)[j]	CAG	TAG	Q3444amber	—
trr-1(n3704)[j]	CAA	TAA	Q694ochre	—
trr-1(n3708)[j]	CGA	TGA	R1248opal	—
trr-1(n3709)[j]	CGA	TGA	R2550opal	—
trr-1(n3712)[j]	TGG	TAG	W2505amber	—

The synMuv proteins described are limited to those for which we obtained mutant allele sequence; this is not a comprehensive listing of synMuv proteins. In the "Wild-type sequence" and "Mutant sequence" columns, exon and intron sequences are denoted by uppercase and lowercase letters, respectively. Nucleotides altered by the mutations are underlined.

[a] Molecular descriptions of the proteins listed were obtained from the following sources: DPL-1, and EFL-1, Ceol and Horvitz (2001) and Page *et al.* (2001); LET-418, Solari and Ahringer (2000) and von Zelewsky *et al.* (2000); LIN-9, Beitel *et al.* (2000); LIN-13, Melendez and Greenwald (2000); LIN-35 and LIN-53, Lu and Horvitz (1998); LIN-36, Thomas and Horvitz (1999) and Reddy and Villeneuve (2004); LIN-52, Thomas *et al.* (2003); MEP-1, Belfiore *et al.* (2002); SLI-1, Yoon *et al.* (1995); MYS-1 and TRR-1, Ceol and Horvitz (2004).

[b] The predicted LET-418 protein contains a sequence that is annotated as a helicase domain (see www.wormbase.org). This domain was originally identified in helicases but has since been found in nonhelicase proteins. Many of these proteins share a common ATPase activity, and this domain contains residues that are important for ATP binding and hydrolysis.

[c] Because of alternative splicing, *trr-1* encodes proteins that may range in length between 4054 and 4064 amino acids (Ceol and Horvitz 2004).

[d] These data are from Figure 1 of Ceol and Horvitz (2001).

[e] These data are from Figure 4 of Ceol and Horvitz (2001).

[f] The adenosine inserted by the *lin-35(n3763)* frameshift mutation is not underlined, because it is unclear which adenosine in the adenosine repeat was inserted.

[g] In addition to the missense mutation described, we found an additional mutation associated with *lin-36(n3765)*. This mutation, AG/gtaagaagaaaagc to AG/gtaagaagaaaagt, is present in the third intron of *lin-36* and creates a possible splice-donor sequence. If this splice-donor were used, an in-frame ochre (TAA) stop codon would be encountered, truncating the LIN-36 protein after 261 amino acids.

[h] These data are from Figure 3 of Thomas *et al.* (2003).

[i] These data are from Figure 2 of Ceol and Horvitz (2004).

[j] These data are from Figure 1 of Ceol and Horvitz (2004).

synMuv genes should be tested more extensively to establish their classifications.

Using more extensive genetic interaction tests and additional criteria to interpret these interactions, we define six classes of genes, synMuv A, synMuv B, synMuv C, *gap-1*, *sli-1*, and *ark-1*, that seem to act in parallel to each other to negatively regulate Ras-mediated vulval development (Table 9). Some of these classes, such as *gap-1*, *sli-1*, and *ark-1*, likely interface directly with Ras pathway components (see below). The point at which the synMuv A, synMuv B, and synMuv C classes interface with Ras signaling is unknown, although recent studies suggest that the synMuv A and synMuv B classes may directly or indirectly repress inappropriate transcription of the Ras pathway activating ligand *lin-3* in the syncytial hypodermis (Cui *et al.* 2006).

Different synMuv gene classes control distinct biochemical activities: A synthetic genetic interaction implies functional redundancy between two sets of genes. There are many possible mechanisms by which two sets of genes might appear redundant. These possibilities include: (1) Two sets of genes encode similar sets of proteins with corresponding proteins of each set controlling the same biochemical activity, and hence each set controls the same biological process; (2) two sets of genes encode distinct sets of proteins with each set controlling distinct biochemical activities but the same biological process; and (3) two sets of genes encode distinct sets of

TABLE 9

Summary of synMuv genetic interactions

Mutation	Phenotype of double mutant with mutation of specified class						Phenotype of double mutant with *let-23*	Inferred synMuv class of mutant gene
	Class A	Class B	Class C	*gap-1*	*sli-1*	*ark-1*		
lin-15A(n767) lin-38(n751)	non-Muv	Muv	Muv	Muv	Muv	Muv	Vul	A
lin-15B(n744) lin-35(n745) lin-65(n3441) mep-1(n3703)[a]	Muv	Non-Muv	Muv	Non-Muv	Non-Muv	Non-Muv	Vul	B
lin(n3628)	Muv	Non-Muv	Non-Muv	Non-Muv	Non-Muv	Non-Muv	Vul	B or *lin(n3628)*[b]
trr-1(n3712)	Muv	Muv	Non-Muv	Muv	Muv	Muv	Vul	C
gap-1(ga133)	Muv	Non-Muv	Muv	NA	Muv	Muv	Non-Vul	*gap-1*
sli-1(n3538)	Muv	Non-Muv	Muv	Muv	NA	Muv	Non-Vul	*sli-1*
ark-1(n3701)	Muv	Non-Muv	Muv	Muv	Muv	NA	Vul	*ark-1*

We provisionally assign 29 genes to six synMuv classes. The assignments of 11 of these genes (shown above and underlined below) are based on extensive genetic interaction tests. The remaining 18 genes have not been tested as extensively. However, on the basis of known genetic interactions and molecular identities, we speculate that most of these 18 genes will remain in the classes to which they have previously been assigned.

Class A: *lin-8*, *lin-15A*, *lin-38*, *lin-56*.
Class B: *lin-9*, *lin-13*, *lin-15B*, *lin-35*, *lin-36*, *lin-37*, *lin-52*, *lin-53*, *lin-54*, *lin-61*, *lin-65*, *dpl-1*, *efl-1*, *hda-1*, *hpl-2*, *let-418*, *lin(n3628)*, *mep-1*.
Class C: *trr-1*, *mys-1*, *epc-1*, *ssl-1*.
gap-1: *gap-1*.
sli-1: *sli-1*.
ark-1: *ark-1*.

NA, not applicable; since each of these classes contains only one gene, double mutants within the same class cannot be constructed.

[a] *mep-1(n3703)* and class C synMuv mutations interact to cause larval lethality at a stage earlier than vulval abnormalities can be determined.

[b] Like class B synMuv mutations, *lin(n3628)* interacts synthetically with class A mutations; does not interact synthetically with class B, *ark-1*, *gap-1*, or *sli-1* mutations; and does not suppress the Vul phenotype of *let-23(sy97)*. However, *lin(n3628)* does not interact synthetically with class C mutations. *lin(n3628)* may define yet another class of synMuv genes. Alternatively, the mutation *n3628* may be a partial loss-of-function mutation too weak to reveal redundancy with class C genes, in which case *lin(n3628)* may be a class B gene. Determination of the *lin(n3628)* null phenotype and genetic interaction tests with a null mutation of this gene should distinguish between these possibilities.

proteins with each set regulating distinct but redundant biological processes.

The first of these mechanisms likely does not apply to the different classes of synMuv genes, as no cloned gene in one synMuv class is similar to any gene of another class. Furthermore, many of the cloned synMuv genes, including the class A gene *lin-15A*, the class B gene *lin-35* Rb, the class C genes *trr-1* and *epc-1*, and *ark-1* and *sli-1*, encode the sole *C. elegans* member of their respective gene families.

The redundancy exhibited among *sli-1*, *gap-1*, and *ark-1* likely exemplifies the second mechanism. *sli-1*, *ark-1*, and *gap-1* are thought to directly downregulate Ras pathway activity, and, as might be predicted on the basis of their synthetic interactions, each is proposed to act upon a different Ras pathway component. *sli-1* encodes a homolog of the c-Cbl proto-oncoprotein, which is thought to downregulate receptor tyrosine kinase levels though ubiquitin-mediated degradation (Yoon *et al.* 1995; Levkowitz *et al.* 1999). *ark-1* encodes a protein that interacts with the SEM-5 SH2/SH3 adaptor protein and is predicted to be a cytoplasmic tyrosine kinase (Hopper *et al.* 2000). Since *sem-5* acts downstream of the *let-23* receptor tyrosine kinase, *ark-1* is proposed to inhibit *let-60* Ras signaling downstream of *let-23*. *gap-1* is a member of the GTPase-activating protein (GAP) family (Hajnal *et al.* 1997). GAPs enhance the catalytic function of Ras family GTPases such as *let-60* Ras, thereby facilitating the switch from active GTP-bound to inactive GDP-bound Ras. The genetic suppression of *let-23(sy97)* by and the molecular identities of *sli-1* and *gap-1* support their action downstream of the *let-23*

receptor tyrosine kinase. Although *ark-1* mutations do not suppress *let-23(sy97)*, Hopper *et al.* (2000) found that an *ark-1* mutation suppressed the Vul phenotypes caused by weaker *let-23* mutations and by *sem-5* mutations. On the basis of these suppression data and the molecular data described above, these authors argued that *ark-1* acts downstream of *let-23*, although its negative regulation of the *let-60* pathway may not be as great as that of *sli-1* or *gap-1*. The redundancy displayed by *sli-1*, *gap-1*, and *ark-1* suggests that a mutation affecting one of these genes only mildly affects Ras pathway activity whereas mutations affecting two genes elevate pathway activity to a level that inappropriately transforms vulval cell fates. That these genes converge on the same signaling pathway implies that they regulate the same biological process.

The class A, B, and C synMuv genes may or may not act similarly. It is possible that these classes act on components of the *let-60* Ras pathway. Since at least some class A and B synMuv genes are thought to act in the hypodermis, an effect on *let-60* Ras signaling is likely indirect and may involve transcriptional regulation of the *lin-3* ligand (Herman and Hedgecock 1990; Hedgecock and Herman 1995; Myers and Greenwald 2005; Cui *et al.* 2006). Alternatively, as in the case of the third mechanism, these classes may regulate entirely distinct biological processes. For example, the class B genes, some of which encode components of a putative histone deacetylase complex, may repress transcription of genes that indirectly promote P(3–8).p cell division. By contrast, the class C genes, which encode components of a putative histone acetyltransferase complex, may activate the transcription of genes, different from those targeted by class B genes, that promote differentiation of P(3–8).p descendants into hypodermal and not vulval cells. A better understanding of synMuv target genes should help to resolve whether different synMuv classes regulate the same or distinct biological activities.

We thank Beth Castor, Na An, and Andrew Hellman for expert technical assistance and Erik Andersen and Adam Saffer for critical reading of this manuscript. We thank Yuji Kohara for providing cDNA clones, Mike Boxem and Sander van den Heuvel for providing pMB1 and pMB7, Min Han for providing pTG96, and Neil Hopper and Paul Sternberg for providing the *ark-1(sy247)* strain. Some of the strains used in this work were provided by Theresa Stiernagle of the Caenorhabditis Genetics Center, which is supported by the National Institutes of Health (NIH) National Center for Research Resources. This work was supported by NIH grant GM24663 to H.R.H., a Koch graduate fellowship to C.J.C., and a Howard Hughes Medical Institute predoctoral fellowship to M.M.H. H.R.H. is the David H. Koch Professor of Biology at Massachusetts Institute of Technology and an Investigator of the Howard Hughes Medical Institute.

LITERATURE CITED

Altschul, S. F., W. Gish, W. Miller, E. W. Myers and D. J. Lipman, 1990 Basic local alignment search tool. J. Mol. Biol. **215:** 403–410.

Anderson, P., 1995 Mutagenesis, pp. 31–58 in *Caenorhabditis elegans: Modern Biological Analysis of an Organism* (*Methods in Cell Biology*, Vol. 48), edited by H. F. Epstein and D. C. Shakes. Academic Press, New York.

Aroian, R. V., and P. W. Sternberg, 1991 Multiple functions of *let-23*, a *Caenorhabditis elegans* receptor tyrosine kinase gene required for vulval induction. Genetics **128:** 251–267.

Austin, J., and J. Kimble, 1989 Transcript analysis of *glp-1* and *lin-12*, homologous genes required for cell interactions during development of *C. elegans*. Cell **58:** 565–571.

Beitel, G. J., S. G. Clark and H. R. Horvitz, 1990 *Caenorhabditis elegans ras* gene *let-60* acts as a switch in the pathway of vulval induction. Nature **348:** 503–509.

Beitel, G. J., E. J. Lambie and H. R. Horvitz, 2000 The *C. elegans* gene *lin-9*, which acts in an Rb-related pathway, is required for gonandal sheath cell development and encodes a novel protein. Gene **254:** 253–263.

Belfiore, M., L. D. Mathies, P. Pugnale, G. Moulder, R. Barstead *et al.*, 2002 The MEP-1 zinc-finger protein acts with MOG DEAH box proteins to control gene expression via the *fem-3* 3′ untranslated region in *Caenorhabditis elegans*. RNA **8:** 725–729.

Brenner, S., 1974 The genetics of *Caenorhabditis elegans*. Genetics **77:** 71–94.

C. elegans Sequencing Consortium, 1998 Genome sequence of the nematode *C. elegans*: a platform for investigating biology. Science **282:** 2012–2018.

Ceol, C. J., and H. R. Horvitz, 2001 *dpl-1* DP and *efl-1* E2F act with *lin-35* Rb to antagonize Ras signaling in *C. elegans* vulval development. Mol. Cell **7:** 461–473.

Ceol, C. J., and H. R. Horvitz, 2004 A new class of *C. elegans* synMuv genes implicates a Tip60/NuA4-like HAT complex as a negative regulator of Ras signaling. Dev. Cell **6:** 563–576.

Chen, Z., and M. Han, 2001 *C. elegans* Rb, NuRD, and Ras regulate *lin-39*-mediated cell fusion during vulval fate specification. Curr. Biol. **11:** 1874–1879.

Clark, D. V., and D. L. Baillie, 1992 Genetic analysis and complementation by germ-line transformation of lethal mutations in the *unc-22* IV region of *Caenorhabditis elegans*. Mol. Gen. Genet. **232:** 97–105.

Clark, S. G., A. D. Chisholm and H. R. Horvitz, 1993 Control of cell fates in the central body region of *C. elegans* by the homeobox gene *lin-39*. Cell **74:** 43–55.

Clark, S. G., X. Lu and H. R. Horvitz, 1994 The *Caenorhabditis elegans* locus *lin-15*, a negative regulator of a tyrosine kinase signaling pathway, encodes two different proteins. Genetics **137:** 987–997.

Cui, M., J. Chen, T. R. Myers, B. J. Hwang, P. W. Sternberg *et al.*, 2006 SynMuv genes redundantly inhibit *lin-3/EGF* expression to prevent inappropriate vulval induction in *C. elegans*. Dev. Cell **10:** 667–672.

Davison, E. M., M. M. Harrison, A. J. Walhout, M. Vidal and H. R. Horvitz, 2005 *lin-8*, which antagonizes *Caenorhabditis elegans* Ras-mediated vulval induction, encodes a novel nuclear protein that interacts with the LIN-35 Rb protein. Genetics **171:** 1017–1031.

Dibb, N. J., D. M. Brown, J. Karn, D. G. Moerman, S. L. Bolten *et al.*, 1985 Sequence analysis of mutations that affect the synthesis, assembly and enzymatic activity of the *unc-54* myosin heavy chain of *Caenorhabditis elegans*. J. Mol. Biol. **183:** 543–551.

Edgley, M. L., and D. L. Riddle, 2001 LG II balancer chromosomes in *Caenorhabditis elegans*: *mT1(II;III)* and the *mIn1* set of dominantly and recessively marked inversions. Mol. Genet. Genomics **266:** 385–395.

Eisenmann, D. M., and S. K. Kim, 1997 Mechanism of activation of the *Caenorhabditis elegans ras* homologue *let-60* by a novel, temperature-sensitive, gain-of-function mutation. Genetics **146:** 553–565.

Ferguson, E. L., and H. R. Horvitz, 1985 Identification and characterization of 22 genes that affect the vulval cell lineages of the nematode *Caenorhabditis elegans*. Genetics **110:** 17–72.

Ferguson, E. L., and H. R. Horvitz, 1989 The multivulva phenotype of certain *Caenorhabditis elegans* mutants results from defects in two functionally redundant pathways. Genetics **123:** 109–121.

Ferguson, E. L., P. W. Sternberg and H. R. Horvitz, 1987 A genetic pathway for the specification of the vulval cell lineages of *Caenorhabditis elegans*. Nature **326:** 259–267.

Frankfort, B. J., and G. Mardon, 2002 R8 development in the *Drosophila* eye: a paradigm for neural selection and differentiation. Development **129:** 1295–1306.

Freeman, M., and J. B. Gurdon, 2002 Regulatory principles of developmental signaling. Annu. Rev. Cell Dev. Biol. **18:** 515–539.

Greenwald, I. S., and H. R. Horvitz, 1980 *unc-93(e1500)*: a behavioral mutant of *Caenorhabditis elegans* that defines a gene with a wild-type null phenotype. Genetics **96:** 147–164.

Hajnal, A., C. W. Whitfield and S. K. Kim, 1997 Inhibition of *Caenorhabditis elegans* vulval induction by *gap-1* and by *let-23* receptor tyrosine kinase. Genes Dev. **11:** 2715–2728.

Han, M., and P. W. Sternberg, 1990 *let-60*, a gene that specifies cell fates during *C. elegans* vulval induction, encodes a ras protein. Cell **63:** 921–931.

Hedgecock, E. M., and R. K. Herman, 1995 The *ncl-1* gene and genetic mosaics of *Caenorhabditis elegans*. Genetics **141:** 989–1006.

Hengartner, M. O., R. E. Ellis and H. R. Horvitz, 1992 *Caenorhabditis elegans* gene *ced-9* protects cells from programmed cell death. Nature **356:** 494–499.

Herman, R. K., 1978 Crossover suppressors and balanced recessive lethals in *Caenorhabditis elegans*. Genetics **88:** 49–65.

Herman, R. K., and E. M. Hedgecock, 1990 Limitation of the size of the vulval primordium of *Caenorhabditis elegans* by *lin-15* expression in surrounding hypodermis. Nature **348:** 169–171.

Hill, R. J., and P. W. Sternberg, 1992 The gene *lin-3* encodes an inductive signal for vulval development in *C. elegans*. Nature **358:** 470–476.

Hodgkin, J., 1997 Appendix 1: genetics, pp. 881–1047 in *C. elegans II*, edited by D. L. Riddle, T. Blumenthal, B. J. Meyer and J. R. Priess. Cold Spring Harbor Laboratory Press, Cold Spring Harbor, NY.

Hopper, N. A., J. Lee and P. W. Sternberg, 2000 ARK-1 inhibits EGFR signaling in *C. elegans*. Mol. Cell **6:** 65–75.

Hsieh, J., J. Liu, S. A. Kostas, C. Chang, P. W. Sternberg *et al.*, 1999 The RING finger/B-box factor TAM-1 and a retinoblastoma-like protein LIN-35 modulate context-dependent gene silencing in *Caenorhabditis elegans*. Genes Dev. **13:** 2958–2970.

Huang, L. S., P. Tzou and P. W. Sternberg, 1994 The *lin-15* locus encodes two negative regulators of *Caenorhabditis elegans* vulval development. Mol. Biol. Cell **5:** 395–411.

Jongeward, G. D., T. R. Clandinin and P. W. Sternberg, 1995 *sli-1*, a negative regulator of *let-23*-mediated signaling in *C. elegans*. Genetics **139:** 1553–1566.

Kimble, J., 1981 Alterations in cell lineage following laser ablation of cells in the somatic gonad of *Caenorhabditis elegans*. Dev. Biol. **87:** 286–300.

Korenjak, M., B. Taylor-Harding, U. K. Binne, J. S. Saterlee, O. Stevaux *et al.*, 2004 Native E2F/RBF complexes contain Myb-interacting proteins and repress transcription of developmentally controlled E2F target genes. Cell **119:** 181–193.

Levkowitz, G., H. Waterman, S. A. Ettenberg, M. Katz, A. Y. Tsygankov *et al.*, 1999 Ubiquitin ligase activity and tyrosine phosphorylation underlie suppression of growth factor signaling by c-Cbl/Sli-1. Mol. Cell **4:** 1029–1040.

Lewis, P. W., E. L. Beall, T. C. Fleischer, D. Georlette, A. J. Link *et al.*, 2004 Identification of a *Drosophila* Myb-E2F2/RBF transcriptional repressor complex. Genes Dev. **18:** 2929–2940.

Lu, X., 1999 Molecular analyses of the class B synthetic multivulva genes of *Caenorhabditis elegans*. Ph.D. Thesis, Massachusetts Institute of Technology, Cambridge, MA.

Lu, X., and H. R. Horvitz, 1998 *lin-35* and *lin-53*, two genes that antagonize a *C. elegans* Ras pathway, encode proteins similar to Rb and its binding protein RbAp48. Cell **95:** 981–991.

Maloof, J. N., and C. Kenyon, 1998 The Hox gene *lin-39* is required during *C. elegans* vulval induction to select the outcome of Ras signaling. Development **125:** 181–190.

Melendez, A., and I. Greenwald, 2000 *Caenorhabditis elegans lin-13*, a member of the LIN-35 Rb class of genes involved in vulval development, encodes a protein with zinc fingers and an LXCXE motif. Genetics **155:** 1127–1137.

Mello, C. C., J. M. Kramer, D. Stinchcomb and V. Ambros, 1991 Efficient gene transfer in *C. elegans*: extrachromosomal maintenance and integration of transforming sequences. EMBO J. **10:** 3959–3970.

Meneely, P. M., and R. K. Herman, 1979 Lethals, steriles and deficiencies in a region of the X chromosome of *Caenorhabditis elegans*. Genetics **92:** 99–115.

Moghal, N., and P. W. Sternberg, 2003 The epidermal growth factor system in *Caenorhabditis elegans*. Exp. Cell Res. **284:** 150–159.

Myers, T. R., and I. Greenwald, 2005 *lin-35* Rb acts in the major hypodermis to oppose Ras-mediated vulval induction in *C. elegans*. Dev. Cell **8:** 117–123.

Page, B. D., S. Guedes, D. Waring and J. R. Priess, 2001 The *C. elegans* E2F- and DP-related proteins are required for embryonic asymmetry and negatively regulate Ras/MAPK signaling. Mol. Cell **7:** 451–460.

Poulin, G., Y. Dong, A. G. Fraser, N. A. Hopper and J. Ahringer, 2005 Chromatin regulation and sumoylation in the inhibition of Ras-induced vulval development in *Caenorhabditis elegans*. EMBO J. **24:** 2613–2623.

Reddy, K. C., and A. M. Villeneuve, 2004 *C. elegans* HIM-17 links chromatin modification and competence for initiation of meiotic recombination. Cell **118:** 439–452.

Robinett, C. C., A. Straight, G. Li, C. Wilhelm, G. Sudlow *et al.*, 1996 *In vivo* localization of DNA sequences and visualization of large-scale chromatin organization using Lac operator/repressor recognition. J. Cell Biol. **135:** 1685–1700.

Rogalski, T. M., D. G. Moerman and D. L. Baillie, 1982 Essential genes and deficiencies in the *unc-22* IV region of *Caenorhabditis elegans*. Genetics **102:** 725–736.

Rosenbluth, R. E., and D. L. Baillie, 1981 The genetic analysis of a reciprocal translocation, *eT1(III; V)*, in *Caenorhabditis elegans*. Genetics **99:** 415–428.

Sigurdson, D. C., G. J. Spanier and R. K. Herman, 1984 *Caenorhabditis elegans* deficiency mapping. Genetics **108:** 331–345.

Solari, F., and J. Ahringer, 2000 NURD-complex genes antagonise Ras-induced vulval development in *Caenorhabditis elegans*. Curr. Biol. **10:** 223–226.

Sternberg, P. W., and H. R. Horvitz, 1986 Pattern formation during vulval development in *C. elegans*. Cell **44:** 761–772.

Sulston, J. E., and H. R. Horvitz, 1977 Post-embryonic cell lineages of the nematode, *Caenorhabditis elegans*. Dev. Biol. **56:** 110–156.

Thomas, J. H., and H. R. Horvitz, 1999 The *C. elegans* gene *lin-36* acts cell autonomously in the *lin-35* Rb pathway. Development **126:** 3449–3459.

Thomas, J. H., C. J. Ceol, H. T. Schwartz and H. R. Horvitz, 2003 New genes that interact with *lin-35* Rb to negatively regulate the *let-60 ras* pathway in *Caenorhabditis elegans*. Genetics **164:** 135–151.

Unhavaithaya, Y., T. H. Shin, N. Miliaras, J. Lee, T. Oyama *et al.*, 2002 MEP-1 and a homolog of the NURD complex Mi-2 act together to maintain germline-soma distinctions in *C. elegans*. Cell **111:** 991–1002.

von Zelewsky, T., F. Palladino, K. Brunschwig, H. Tobler, A. Hajnal *et al.*, 2000 The *C. elegans* Mi-2 chromatin-remodelling proteins function in vulval cell fate determination. Development **127:** 5277–5284.

Wang, B. B., M. M. Muller-Immergluck, J. Austin, N. T. Robinson, A. Chisholm *et al.*, 1993 A homeotic gene cluster patterns the anteroposterior body axis of *C. elegans*. Cell **74:** 29–42.

Wicks, S. R., R. T. Yeh, W. R. Gish, R. H. Waterston and R. H. Plasterk, 2001 Rapid gene mapping in *Caenorhabditis elegans* using a high density polymorphism map. Nat. Genet. **28:** 160–164.

Williams, B. D., B. Schrank, C. Huynh, R. Shownkeen and R. H. Waterston, 1992 A genetic mapping system in *Caenorhabditis elegans* based on polymorphic sequence-tagged sites. Genetics **131:** 609–624.

Yoon, C. H., J. Lee, G. D. Jongeward and P. W. Sternberg, 1995 Similarity of *sli-1*, a regulator of vulval development in *C. elegans*, to the mammalian proto-oncogene *c-cbl*. Science **269:** 1102–1105.

Zorio, D. A., N. N. Cheng, T. Blumenthal and J. Spieth, 1994 Operons as a common form of chromosomal organization in *C. elegans*. Nature **372:** 270–272.

Communicating editor: B. J. Meyer